Dynamics of Ubiquitin-Conjugate Population in Response to Inhibition of Ubiquitin-Proteasome Pathway

Dynamics of Ubiquitin-Conjugate Population in Response to Inhibition of Ubiquitin-Proteasome Pathway

James J. Minissale

A Thesis in the Field of Biology

for the Degree of Master of Liberal Arts in Extension Studies

Harvard University

November 2018

Abstract

The goal of this research was to evaluate the dynamics of ubiquitin-protein conjugate populations in response to treatment with inhibitors of the ubiquitin-proteasome pathway. The 26S proteasome is a large multimolecular complex found in all eukaryotic cells that is responsible for regulating protein levels through degradation. Ubiquitin-activating enzyme (UAE) is one of two E1 enzymes that activate ubiquitin upstream of the proteasome and is the primary enzyme responsible for labeling proteins for degradation by the proteasome. Chemical or genetic inhibition of UAE activity leads to an accumulation of proteins that are normally turned over by the proteasome. Little is known about the population-level response of ubiquitinated proteins to inhibition of UAE and the proteasome. In the work described in this thesis, the subpopulations of ubiquitin-linkage type were assessed by cellular colocalization assays and quantitative mass spectrometry in bortezomib, a proteasome inhibitor, and TAK-243, a UAE inhibitor, treated cells in culture. Immunofluorescence localization data suggests the ubiquitin conjugates that accumulate in perinuclear aggregates are the only conjugates that persist in response to TAK-243 treatment (i.e. are resistant to DUBs). Furthermore, the data suggests that all linkage types of ubiquitin conjugates stochastically accumulate in response to bortezomib and then a fraction of these aggregate in perinuclear bodies in a form that is resistant to degradation or deubiquitination.

Acknowledgments

I would like to recognize the support of several people who assisted me in the preparation of this document. I would like to thank my advisors Dr. Lawrence Dick and Dr. Alfred Goldberg for their guidance and review of this work. I would also like to thank Dr. James Morris for his support and oversight. I would like to thank Dr. Teresa Soucy, my manager for her motivation and guidance initiating this project. I would like to thank many of my colleagues Dr. Xiaofeng Yang, Dr. Hongbo Gu, Dr. Janice Lee, Angel Maldonado-Lopez, Claudia Rabino, and Dr. Neil Rollins, for their contributions and guidance in completion of this work. And finally I would like to thank my wife, Elena Minissale, and my son, Frank Peter Minissale, for their motivation, inspiration, love, and support during this long process. Without them this endeavor may never have succeeded.

Table of Contents

Acknowledgments iv

List of Tables vii

List of Figures/Graphs viii

I. Introduction 1

Cancer and Multiple Myeloma 1

Ubiquitin Proteasome Pathway 2

Unfolded Protein Response 8

Bortezomib and TAK-243 10

II. Materials and Methods 13

Cell Culture 13

Immunoblot 13

Immunofluorescence 14

Aggresome Detection Assay 15

Mass Spectrometry 16

III. Results 17

Ubiquitin Conjugate Response to UAE Inhibition and Proteasome Inhibition 17

Formation of Perinuclear Aggregates with Prolonged Proteasome Inhibition 18

Mass Spectrometry 19

IV. Discussion 21

Significance of Results 21

Study Limitations 23

Direction of Future Research 25

Conclusions 26

Appendix 27

References 39

List of Tables

Table 1. Relative amount of ubiquitin linkage types in SKOV3 cells treated with bortezomib and/or TAK-243..... 28

List of Figures

Figure 1. Overview of the enzymatic cascade involved a ubiquitin-like protein (UBL) conjugation and the ubiqitin–proteasome system (UPS) 3

Figure 2. Overview of ubiquitin linkage topology 4

Figure 3. Representative diagram of the proteasome 6

Figure 4. Overview of eight E1 activating enzyme cascades 8

Figure 5. The PERK, IRE1, and ATF6 unfolded protein response pathways 9

Figure 6. Total ubiquitin conjugate levels of SKOV3 cells treated with a dose response of TAK-243 29

Figure 7. Quantitation and normalization of total ubiquitin conjugate levels of SKOV3 cells treated with bortezomib or TAK-243 30

Figure 8. K48-ubiquitin conjugate levels of SKOV3 cells treated with a dose response of TAK-243 31

Figure 9. Quantitation and normalization of K48- ubiquitin conjugate levels of SKOV3 cells treated with bortezomib or TAK-243 32

Figure 10. Western blot analysis of SKOV3 cells treated with 0.5 μM of TAK-243 or 0.5μM bortezomib 33

Figure 11. Bortezomib induces perinuclear aggregate formation which TAK-243 does not appear to modulate 34

Figure 12. Ubiquitin conjugates in perinuclear aggregate inclusion bodies are not reduced by TAK-243 treatment 35

Figure 13. Strong, diffuse Ub-K48 signal is observed with bortezomib treatment alone that decreases when cells are subsequently treated with TAK-243 36
Figure 14. Strong, diffuse Ub-K48 signal is observed with bortezomib treatment alone that decreases when cells are subsequently treated with TAK-243 for 24 hours 37
Figure 15. Relative amounts of ubiquitin linkages observed in SKOV3cells pretreated with bortezomib and/or TAK-243 as measured by mass spectrometry 38

Chapter I

Introduction

Cancer and Multiple Myeloma

Cancer is a disease of uncontrolled cell growth ("What Is Multiple Myeloma?" 2018). While there is much variety in cancer types and origins, cancer development is generally believed to be the result of a multistep process of genetic alteration (Hanahan & Weinberg, 2011). The accumulation of genetic alterations which interfere in key cellular processes leads to the transformation of normal tissue into cancerous tissue (Hanahan & Weinberg, 2011).

Multiple myeloma is a type of cancer derived from plasma cells and is the second most prevalent form of blood cancer (Driscoll et al., 2010). Plasma cells are responsible for generating antibodies and as such, their normal function depends on the ubiquitin proteasome system to remove by degradation misfolded or excess antibody subunits. In normal cells, this natural load of degradation is handled by the ubiquitin-proteasome system. However, it has been suggested that in the case of cancer cells accumulation of genetic abnormalities may increase the likelihood of misfolded or overexpressed proteins that would need to be degraded (Deshaies, 2014). Some evidence suggests that this can lead to a state of proteotoxic stress where a cancer cell would be more dependent on protein homeostasis mechanisms, such as the UPS (Obeng et al., 2006; Deshaies, 2014). This increased dependence on protein quality control represents a proven therapeutic target for small molecule inhibitors of this pathway.

Ubiquitin Proteasome Pathway

Ubiquitin is a small protein that can be conjugated post translationally to other proteins to play an essential role in a wide range of cellular processes including: cell signaling, protein homeostasis, proliferation, and DNA damage repair (Bedford et al., 2011; Driscoll et al., 2010; Schulman & Harper, 2009). Conjugating ubiquitin to a protein substrate is a multistep process that is initiated by the primary ubiquitin-activating enzyme (UAE or E1; Haas, 1982). The mechanism of UAE consists of three steps shown in Figure 1 below (Bedford et al., 2011). First, UAE binds ubiquitin and ATP and catalyzes the formation of a ubiquitin adenylate intermediate, releasing inorganic phosphate. Next, the catalytic cysteine residue in UAE attacks the adenylate to form a covalent thioester intermediate (UAE~ubiquitin), releasing AMP as the by-product. Finally, the UAE~ubiquitin thioester binds another molecule of ATP and ubiquitin to form another ubiquitin adenylate, forming a UAE complex with a ubiquitin thioester and a ubiquitin adenylate present. This UAE ternary complex is now capable of transferring the charged ubiquitin thioester to the catalytic cysteine of an E2 in a transthiolation reaction. The ubiquitin-charged E2 then binds to one of many E3 ligases which facilitates the covalent attachment of ubiquitin to a substrate via a lysine residue (Haas et al., 1982; Schulman & Harper, 2009; Bedford et al., 2011).

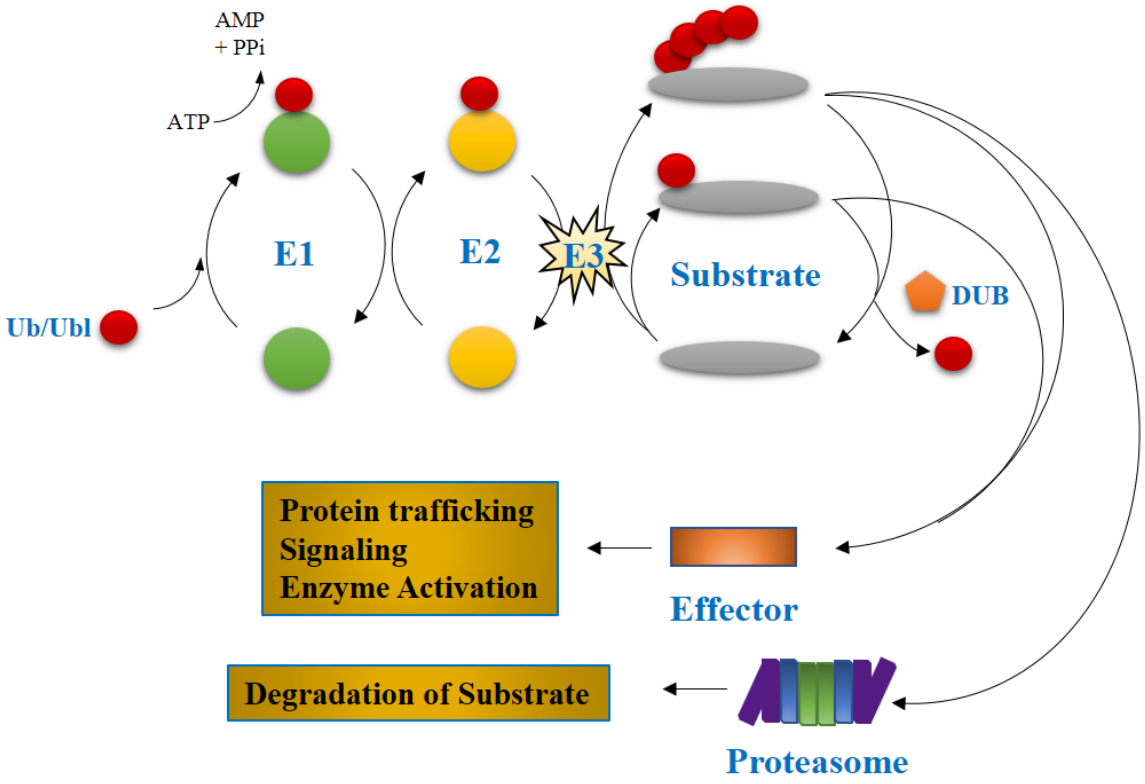

Figure 1. Overview of the enzymatic cascade involved a ubiquitin-like protein (UBL) conjugation and the ubiqitin–proteasome system (UPS). Ubiquitin-activating enzyme (E1) binds ATP and ubiquitin (Ub) to form a ternary complex consisting of E1–ubiquitin thioester with ubiquitin–AMP bound. The thioester-bound ubiquitin is then passed to one of several E2 conjugating enzymes through a transthiolation reaction. The ubiquitin-charged E2 then forms a complex with an E3 ligase and a protein substrate to transfer ubiquitin to a lysine residue on the substrate or contribute to a preexisting ubiquitin on the substrate. Mono- and poly-ubiquitinated substrates can interact with various effector proteins to serve as a cellular signaling mechanism. Likewise, a chain of K48-linked ubiquitins can mark substrates for degradation. Following release from the E3, the proteasome recognizes the polyubiquitin chain, and the substrate is deubiquitylated and destroyed. Figure adapted from Bedford et al., 2011.

Ubiquitination can convey a variety of context-dependent signals. A substrate can be modified with a polyubiquitin chain formed by linking ubiquitins together or monoubiquitin. Ubiquitin chains can be formed through one its seven lysines or a linear chain can be formed through methionine-1 linkages. Each linkage type confers a different topology to the

polyubiquitin chain and a mixture of different linkages can be found in a single chain (Messick & Greenberg, 2009; Swatek & Komander, 2016). In humans, lysine-48 (K48) linked polyubiquitin chains are the best characterized and signal the modified substrate protein for degradation by the proteasome. Modified ubiquitin and ubiquitin chains formed from other ubiquitin lysine linkages have been shown to be involved in signaling pathways, protein localization, and enzyme activity (Kim et al., 2011; Haglund et al., 2003; Bedford et al., 2011; Swatek & Komander, 2016).

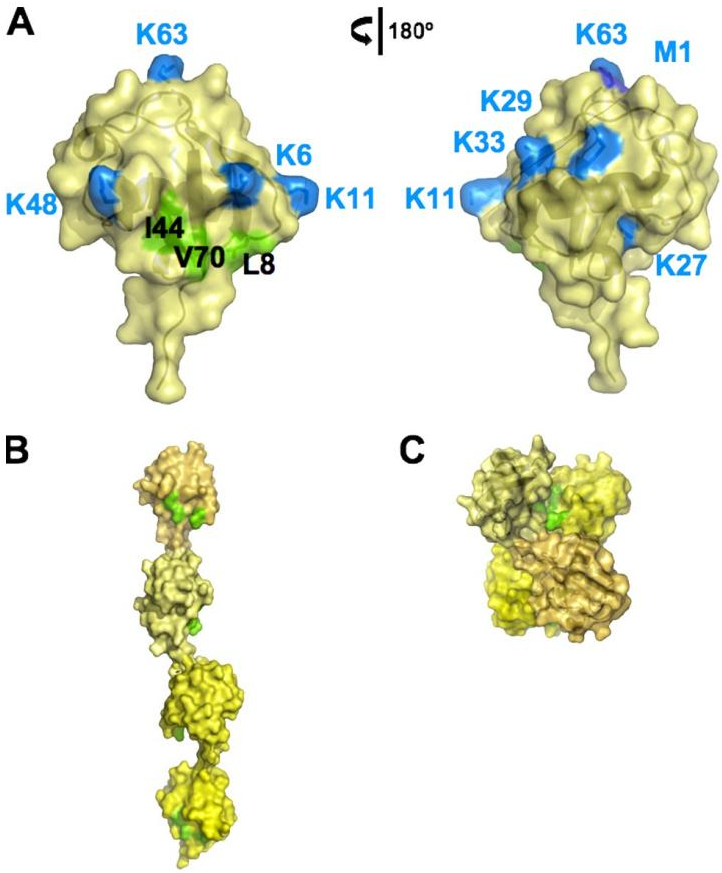

Figure 2. Overview of ubiquitin linkage topology. A) surface representation of ubiquitin with seven lysines and N-terminal methionine responsible for polyubiquitin chain formation are shown in blue. Hydrophobic patch responsible for many ubiquitin binding interactions is shown in green. B) Model of K63-tetraubiquitin chain C) Model of K48-tetraubiquitin chain. Conformational differences between linkage types are capable of conveying signals through a variety of physiological pathways. Figure from Messick & Greenberg, 2009.

The proteasome is a large multimeric complex consisting of a 20S core particle and one or more 19S regulatory particles. The hollow 20S core contains the proteolytic activity of the proteasome and consists of two copies each of a seven-subunit outer rings containing α-subunits and a seven-subunit inner rings containing β-subunits. The β1, β2, and β5 subunits contain the caspase-like, trypsin-like, and chymotrypsin-like proteolytic activity responsible for protein degradation (Kisselev et al., 2006). The 19S regulatory particle is responsible for binding, unfolding, and feeding ubiquitinated substrates into the 20S core. It can be subdivided into the base and the lid. The base contains two scaffolding proteins Rpn1 and Rpn2, a ubiquitin receptor Rpn13, and a heterohexameric AAA+ ATPase ring. Rpt1-6, that interacts with the 20S core and is responsible for opening the α-ring pore and unfolding the substrate protein. The lid contains another ubiquitin receptor, Rpn10, a deubiquitinase, Rpn11, and seven other proteins involved in coordinating the complex machinery of the 19S cap (Kisselev et al., 2006; Blackburn et al., 2010). Once a substrate protein is tethered to the 19S regulatory particle by its polyubiquitin chain the protein is unfolded, the ubiquitin chains are removed, fed into the 20S core particle, and the protein is degraded (Deshaies, 2014; Beckwith et al., 2013). The proteasome also has ubiquitin-independent proteolytic activity that involves other regulatory particles, such as PA28γ and PA200 (Sanchez-Lanzas & Castano, 2014).

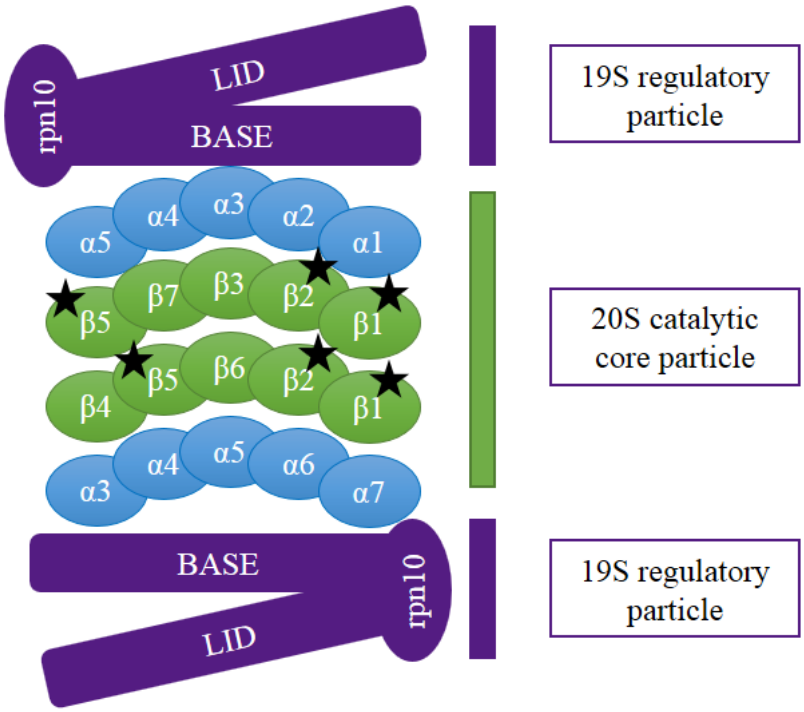

Figure 3. Representative diagram of the proteasome. The 19S regulatory particle consists of lid and base components that unfold and feed the ubiquitinated substrate into the core. The 20S core particle consists of two copies of identical seven-subunit rings. The proteolytic function is found in the β1, β2, and β5 subunits found in the inner two rings (stars). Figure adapted from Cottini et al., 2014.

Ubiquitin can also be removed from a substrate by a class of enzymes known as deubiquitinases (DUBs). This process is believed to exist in a regulated equilibrium where DUBs are removing ubiquitin molecules added by a substrates cognate E3 (Reyes Turcu, Ventii, & Wilkinson, 2009). DUBs are also responsible for activation of ubiquitin from a premature form and recycling free, unanchored ubiquitin chains into ubiquitin monomers to restore ubiquitin supply. There are five families of DUB that have different specificities and roles in the cell (Reyes Turcu, Ventii, & Wilkinson, 2009). These families are ubiquitin C-terminal hydrolases (UCH), ubiquitin specific protease (USP), ovarian tumor (OTU), Josephin domain, and

JAB1/MPN/Mov34 metalloenzyme (JAMM) domain. JAMM domain DUBs are a family of metalloproteases while the four other classes are papain-like cysteine proteases (Reyes Turcu, Ventii, & Wilkinson, 2009). Usp14 is a proteasome-associated DUB which can regulate 26S function by disassembling ubiquitin chains on proteins proximal to the proteasome, rescuing them from degradation (Lee et al., 2016). Rpn11/POH1 is a JAMM domain DUB in the 19S cap of the proteasome responsible for controlling access to the proteasome by removing ubiquitin chains from proteins and allowing them to enter the proteasome. Disregulation of POH1 activity has been shown to be involved in tumorigenesis and cancer cell survival (Wang et al., 2015).

In humans, there are eight E1 activating enzymes and more than a dozen ubiquitin-like proteins (UBLs) that play important roles in regulating diverse biological pathways (Figure 4, Bedford et al., 2011; Schulman & Harper, 2009). Other E1 enzymes activate their cognate UBLs through a similar multistep process as UAE (Schulman & Harper, 2009). Ubiquitin is the only UBL known to be activated by two E1s, UAE and Uba6 (also known as Ube1L2). Uba6 selectively activates Ubiquitin and a related UBL, FAT10 and transfers them to a unique E2, USE1 (Uba6-specific E2). Despite this similarity, the role of Uba6 is distinct from that of UAE in that, unlike UAE, it is not required for viability *in vitro* (Schulman & Harper, 2009).

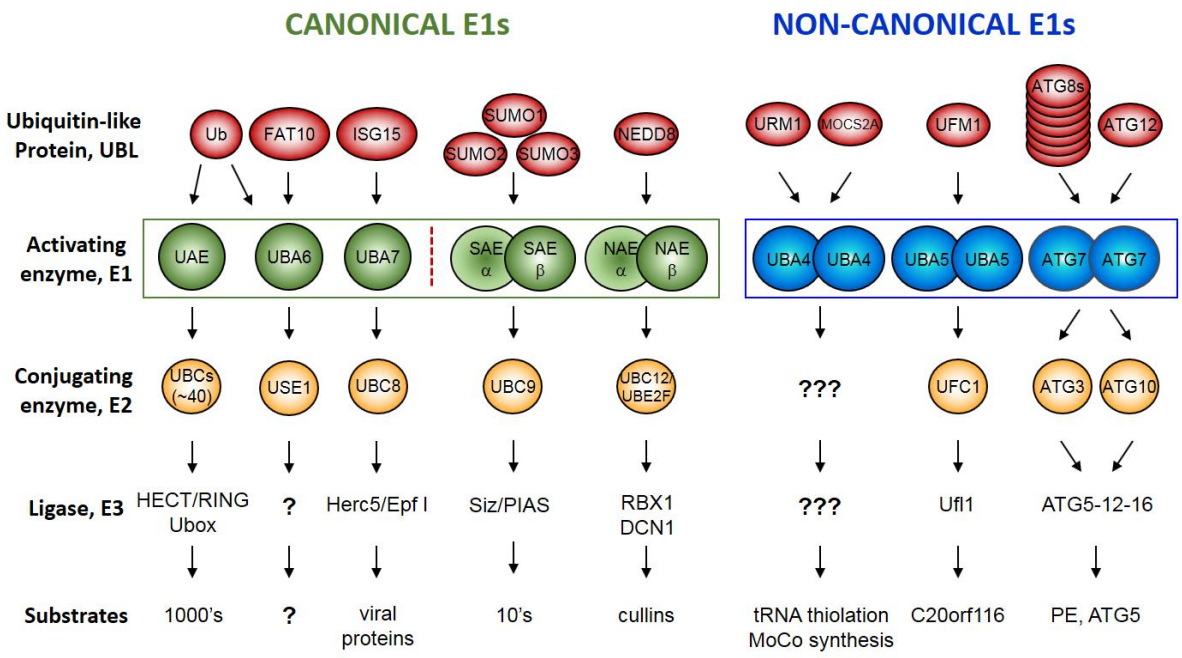

Figure 4. Overview of eight E1 activating enzyme cascades involved in ubiquitin-like protein conjugation. E1s, E2s, and UBLs are structurally and mechanistically related but are involved in diverse biological pathways. Generally, UBLs are unique substrates of their cognate E1 with ubiquitin being the exception as it can be conjugated by UAE and Uba6. Figure and legend adapted from Bedford et al., 2011.

Unfolded Protein Response

Disruption of normal protein homeostasis activates a protective response to isolate, repair, or remove accumulating aberrant proteins. The unfolded protein response can be activated by three endoplasmic reticulum (ER) proteins; activating transcription factor (ATF6), inositol requiring kinase 1 (IRE1α), and PKR-like ER kinase (PERK) resulting in up-regulation of genes for ER chaperones involved in protein folding, for components of the protein degradation machinery, and for proteins involved in apoptosis (Ri et al., 2016). The ER is where newly synthesized membrane and secretory proteins are folded, glycosylated and transported. The objective of this ER stress response is to reduce protein translation, increase ER functional

capacity, and increase ER-associated degradation (ERAD) components (Ri et al., 2016). One such component of ERAD is the ubiquitin-proteasome pathway. When UPR pathways are activated, aberrant proteins are removed from the ER and subjected to ubiquitination and proteasomal degradation. Prolonged activation of ER-stress response pathways ultimately results in apoptosis as the cell is unable to resolve the accumulation of aberrant proteins. Thus, the ubiquitin-proteasome pathway is a critical component for resolving ER-stress through ERAD and helping cells to survive ER-stress (Figure 5; Ri et al., 2016).

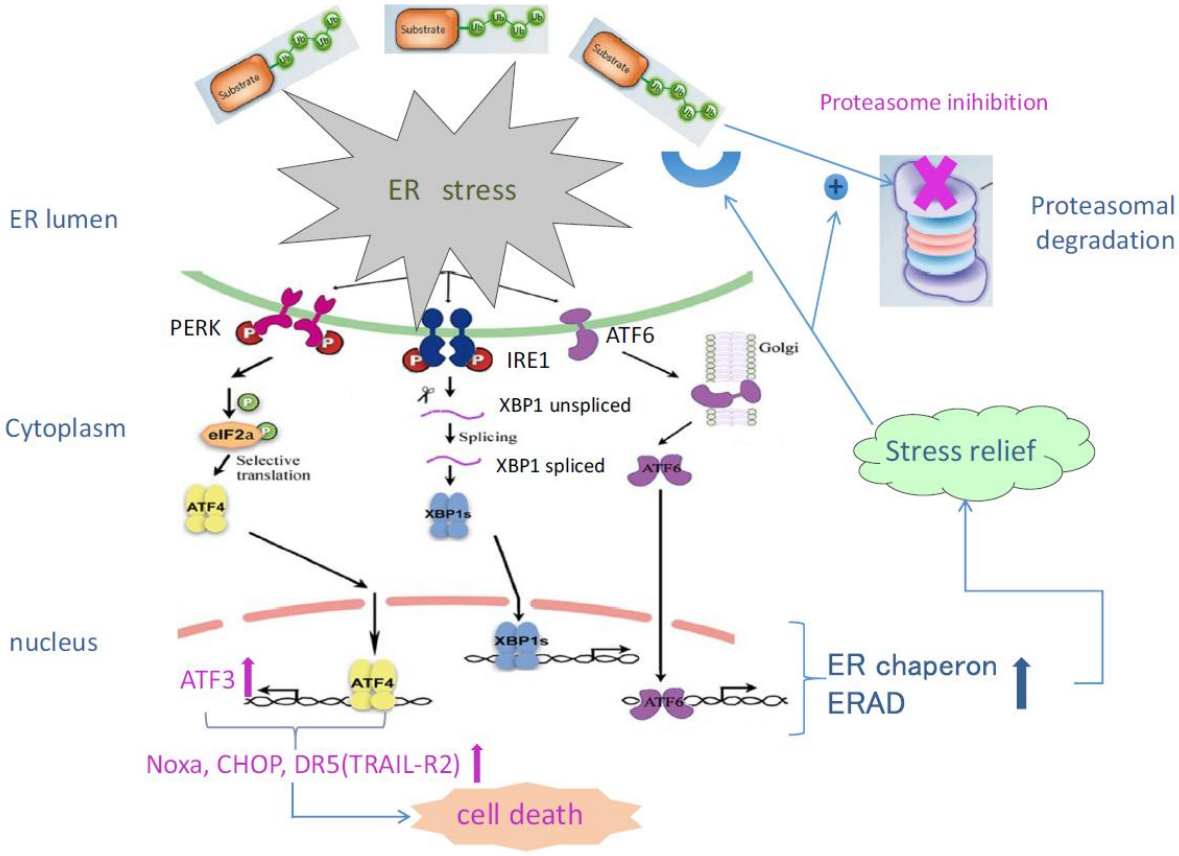

Figure 5. The PERK, IRE1, and ATF6 unfolded protein response pathways can relieve ER stress through upregulation of ER chaperons and ER-associated protein degradation pathways. However, proteasome inhibition triggers can trigger fatal ER stress leading to activation of pro-apoptotic factors including ATF families, Noxa, CHOP, and DR5 (Ri et al., 2016).

Autophagy is a process for both bulk and targeted protein turnover through the formation of double-membrane enclosed autophagasomes which are shuttled to the lysosome for degradation (Rogov et al., 2014). Misfolded and aberrant proteins that have been ubiquitinated can aggregate and form inclusion bodies. Some report this is an organized process that deposits aggregated proteins into distinct inclusion bodies, known as JUNQ and IPOD, at specific cellular sites; particularly in the perinuclear region for JUNQ (Kaganovich et al., 2008). It is unclear if these bodies are an attempt for enhanced ubiquitin conjugate clearance or linked to other cell fates but there is evidence that they play a role in promoting survival before autophagy activation (Sha et al., 2018).

Bortezomib and TAK-243

VELCADE® (bortezomib) is a type of chemotherapy called a targeted therapy. It is approved by the FDA for the treatment of multiple myeloma and mantle cell lymphoma ("How How VELCADE® (bortezomib) works", 2016). It is a potent covalent and reversible small-molecule inhibitor of the β5 subunit of the 26S proteasome (Blackburn et al., 2010). It has been shown to have broad cytotoxicity in human tumor cell types *in vitro* and Bortezomib-induced proteotoxic stress leads to cell death by interfering with a number of critical cell pathways including ribosomal function, polyamine homeostasis, protein translation initiation, and DNA damage signaling and response (Blackburn et al., 2010; Chen et al., 2010). The efficacy of bortezomib in the treatment of multiple myeloma is believed to be due to the high levels of proteotoxic stress induced in plasma cells, which synthesize high levels of antibody subunits, as well as the loss of NFκB activation through stabilization of IκB, a key growth signal which plasma cells rely on (Deshaies, 2014; Goldberg, 2012). Without the ability to degrade the high

levels of overexpressed and misfolded protein, bortezomib-treated myeloma cells undergo proteotoxic crisis leading to cell death (Deshaies, 2014; Nawrocki et al., 2005).

Inhibition of proteasome activity by bortezomib can be monitored in several ways: measurement of global polyubiquitination levels or accumulation of proteasome substrates, *in situ* measurements of proteasome peptidase activity (e.g. Proteasome-Glo assay), accumulation of rapidly turned over reporter gene products (e.g. NFκB-Luc assay, and 4xUb-Luc assay), or simply by measuring effects of proteasome inhibition on cell viability (Blackburn et al., 2010).

TAK-243 is a potent, time-dependent inhibitor of UAE and Uba6 that utilizes the E1 activation mechanism to form a covalent TAK-243-Ubiquitin adduct which tightly associates with UAE in its adenylation domain, blocking enzymatic activity (Hyer et al., 2018). Inhibition of UAE disrupts total cellular protein ubiquitination resulting in disregulation of protein turnover and signaling leading to cell death (Hyer et al., 2018). Although UAE is essential for the survival of all cells, it is believed that tumor cells may have increased sensitivity to TAK-243 as a result of their rapid growth rate, increased metabolic demands, and proteotoxic stress (Hyer et al., 2018).

Inhibition of ubiquitination by TAK-243 is monitored through many of the same markers as proteasome inhibition, including global polyubiquitination status and stabilization of short-lived proteins such as c-Jun, c-Myc, and p53 as well as G2/M cell-cycle arrest, ubiquitination status of mono-ubiquitinated proteins such as PCNA and FANCD2, impaired DNA damage response measured by COMET assay, and cell viability (Hyer et al., 2018). In contrast to proteasome inhibition, TAK-243 treatment leads to a rapid decrease in polyubiquitin levels. This is because blocking ubiquitin conjugate synthesis while DUB activity depletes the pool of ubiquitinated proteins. Conversely, inhibition of the proteasome leads to accumulation of normally degraded

protein substrates. It is not clear, however, why inhibition of the proteasome leads to an accumulation of *ubiquitinated* protein substrates, as DUB activity should still continue unabated.

Chapter II

Materials and Methods

Cell Culture

Human colon cancer cells (HCT116) and ovarian cancer cells (SKOV3) were obtained from ATCC and cultured under sterile conditions at Takeda Pharmaceuticals International Co. in BL2 tissue culture labs. Cells were grown in preferred growth media (McCoy's 5A, 10% fetal bovine serum (FBS), 1% L-Glutamine). Cells were treated with proteasome inhibitor, bortezomib, and UAE inhibitor, TAK-243, provided by Takeda Pharmaceuticals.

Immunoblot

For immunoblot studies, HCT116 and SKOV3 cells were seeded in 6 well plates with $2.5x10^5$ cells per well and allowed to sit at 37°C overnight. Cells were pretreated the next day with 20 nM bortezomib or Dimethyl sulfoxide (DMSO) for 24 hours followed by DMSO, bortezomib (20 nM for HCT116 or 500 nM for SKOV3) or TAK-243 (100 nM for HCT116 or 500 nM for SKOV3) for 0, 1, 2, 4, 6, or 24 hours. Cells were then harvested by removing media, washing with phosphate buffered saline (PBS), and scraping into lysis buffer (50 mM Tris pH 7.5, 150 mM sodium chloride (NaCl), 10 mM ethylenediaminetetraacetic acid (EDTA), 1% nonidet P40, 1% (w/v) deoxycholate, 0.1% (v/v) SDS, 1X protease inhibitor cocktail (Roche), 10mM N-ethylmaleimide (NEM), 10 mM Iodoacetamide, 1X benzonase nuclease). Protein concentration was determined by bicinchoninic acid (BCA) assay (BioRad) and normalized in

1X NuPAGE LDS sample buffer (Invitrogen); 100 μg of these cell lysates were set aside for mass spectrometry experiments.

Immunoblots were prepared by running sodium dodecyl sulfate polyacrylamide gel electrophoresis (SDS-PAGE) on 15 μg per sample of cell lysates followed by transfer to a Polyvinylidene fluoride (PVDF) membrane using Trans-Blot Turbo Transfer (BioRad) system as per protocol provided by the manufacturer. Next, PVDF membranes were blocked in 5% (w/v) non-fat dried milk in tris-buffered saline with 0.1% Tween-20 (NFDM/TBST) then stained with linkage-independent or linkage-specific ubiquitin antibodies raised to differentially detect lysine-48 (Apu2, EMD Millipore), lysine-63 (Apu3, EMD Millipore), total ubiquitin chains (FK2, ENZO), or total ubiquitin (P4D1, Santa Cruz). GAPDH (14C10, Cell Signaling Technologies) was included as a loading control. Goat anti-Rabbit and anti-Mouse IgG antibodies conjugated with AlexaFluor 680 were used as secondary antibodies for imaging using an Odyssey LiCOR imager to measure the fluorescent intensity of bands.

Immunofluorescence

Ubiquitinated protein conjugates were also measured by immunofluorescence to monitor cell localization in treated cells. For these studies, HCT116 and SKOV3 cells were seeded in 96 well clear-bottom tissue culture plates (Greiner) at 3000 cells per well and allowed to sit at 37ºC overnight. Cells were then pretreated with DMSO or 20 nM bortezomib and allowed to incubate for another 24 hours. The next day, cells were treated with DMSO or a titration of bortezomib or TAK-243. Compounds were serially diluted 1:2 such that the final concentration ranged from 1 μM - 0.004 μM.

96 well plates were prepared for analysis at 0, 0.25, 0.5, 1, 2, 4, 6, 24, or 48 hours as follows; media was removed from wells and replaced with 4% paraformaldehyde (PFA) to fix cells. After ten minutes, PFA was removed and replaced with 0.5% Triton X-100 for 15 minutes to permeabilize cell membranes. Cells were then incubated for one hour in 0.5% Blocking reagent (Roche) diluted in 100 mM Tris pH 7.5, 150 mM NaCl. Next, cells were incubated with antibodies raised to bind lysine-48 (K48; Apu2, EMD Millipore), lysine-63 (K63; Apu3, EMD Millipore), total ubiquitin (P4D1, Santa Cruz), or total polyubiquitin chains (FK2, ENZO) diluted in Blocking reagent for one hour, washed with PBS, and then incubated with goat anti-mouse and/or anti-rabbit secondary antibodies conjugated with AlexaFluor-488 or AlexaFluor-594. Hoechst dye (Thermo) was included with secondary antibodies to image cell nuclei. Cells were then washed with PBS and images were taken.

Cell images were obtained using an ImageXpress Micro XLS Widefield High-Content Analysis System with a 20x confocal objective and analyzed in MetaExpress to measure average cell intensity using Cell Scoring.

Aggresome Detection Assay

Treated HCT116 and SKOV3 cells were also used to detect total aggregated proteins using the PROTEOSTAT Aggresome Detection kit (Enzo). According to the manufacturer, this kit contains a red fluorescent molecular rotor dye that becomes fluorescent when bound to denatured protein within aggresomes and aggresome-like inclusion bodies in fixed and permeabilized cells. Cells were prepared and imaged as they were for immunofluorescence except as follows; 95% methanol in PBS was used to permeabilize cells instead of 0.5 % Triton X-100 and no antibody steps were required.

Mass Spectrometry

Cell lysates from immunoblot experiments were set aside for Mass Spectrometry to measure the relative amounts of K6, K11, K27, K48, and K63 ubiquitin chains. To perform this analysis with samples prepared for immunoblot, previously treated WSU cell lysates that had been grown for SILAC (stable isotope labeling by amino acids in cell culture) was used. Cells labeled for SILAC were cultured in media containing heavy-isotope labelled arginine and lysine for 5-10 doublings then cell pellets are frozen for future use. The WSU lysates prepared for SILAC were mixed in equal proportion with SKOV3 cell lysates prepared for earlier immunoblot studies and then reduced and alkylated.

Total cellular proteins were resolved by SDS-PAGE as described above. Gel bands above 25 kDa were sliced from the gel and an in-gel digestion was performed using a combination of proteases, Lys-C and Trypsin. Each sample was analyzed on an Orbitrap-Fusion Mass Spectrometer over a 120 minute gradient in targeted MS2 mode focusing on diGly-peptides from each Ubiquitin linkage site (see Table 1).

To obtain the normalized intensity of each ubiquitin linkage type, the ratio of raw intensity of heavy-labeled WSU lysate and light-labeled SKOV3 lysate was measured for the peptide indicating each linkage type. The observed molecular weight in the heavy-labelled WSU lysate is 2 Da greater per lysine and arginine residue than expected due to the heavy-isotope labeling. To get a more representative value of the relative levels of each linkage across samples, the normalized intensity was then multiplied by the ratio of the WSU lysate from the DMSO control over the WSU lysate corresponding to the sample in question.

Chapter III

Results

Ubiquitin Conjugate Response to UAE Inhibition and Proteasome Inhibition

HCT116 and SKOV3 cells were treated with 0.5 μM of either TAK-243 or bortezomib and harvested at 0, 2, 4, 6, or 24 hours to assess the effect of inhibition of UAE and Proteasome on various ubiquitin populations by immunoblot. Antibodies specific to K48 ubiquitin chains, K63 ubiquitin chains, polyubiquitin, and total ubiquitin were used to track ubiquitin populations in treated cells by immunoblot and immunofluorescence. The complete results can be found as Figures in the Appendix.

It was observed that bortezomib treatment induced an accumulation of poly ubiquitin signal and a decrease in mono ubiquitin as measured by total ubiquitin antibodies. This accumulation began as early as 2 hours as observed by immunoblot and continued through the final timepoint taken at, 24 hours (Figure 10). Conversely, TAK-243 treatment led to a complete loss of higher molecular weight polyubiquitin species within 2 hours and an increase in mono ubiquitin that corresponds to the deconjugation of polyubiquitin chains (Figure 10). HCT116 and SKOV3 cells were then seeded for an immunofluorescence time course/dose-response study. Cells were treated with a dose response of compounds from 1 μM to 0.004 μM and timepoints taken at 15, 30, 60, 120, 240 minutes (Figures 6-9). These earlier time points were chosen to give better resolution on the rapid change in ubiquitin populations following treatment; however, HCT116 cell morphology was not well suited to cellular localization analysis. It was observed that SKOV3 cells showed a broadly cytoplasmic staining pattern when looking at polyubiquitin

chains or K48-specific ubiquitin chains. When treated with 0.25 μM bortezomib for more than 2 hours, K48 signal increases broadly while total polyubiquitin conjugates shift from nuclear to cytoplasmic. Meanwhile, a similar treatment of TAK-243 leads to a uniform decrease in K48 signal as well as with total polyubiquitin signal. Unfortunately, conditions were not identified to adequately measure ubiquitin status with chain-specific K63 antibodies and the K48 specific antibodies did not work by immunoblot.

Formation of Perinuclear Aggregates with Prolonged Proteasome Inhibition

Prior work by scientists at Takeda, suggests that longer treatments of low dose bortezomib induces large protein aggregates near the nucleus that stain positive for Ubiquitin, LC3, p62, and HDAC6 (Neil Rollins, personal communication, 2015). To demonstrate the formation of these perinuclear aggregates and identify optimal conditions to reproduce them, SKOV3 cells were treated for 24 hours with a dose-response of bortezomib (Figure 11). Perinuclear aggregates were detected at 24 hours of treatment with 111 nM bortezomib using a PROTEOSTAT aggresome detection kit purchased from ENZO. These samples were then subjected to a subsequent treatment of either DMSO or 1 μM TAK-243 for 1 hour. The complete results can be found as Figures in the Appendix.

As was seen previously, cells treated with bortezomib showed an increase in cytoplasmic staining of polyubiquitin and K48-specific ubiquitin linkages. However, unlike what was observed with the shorter treatments, these cells now exhibit nuclear-adjacent bodies that stain positive for total polyubiquitin and K48 specific ubiquitin linkages (Figure 12).

To assess if there was a time dependent component to a potential TAK-243-dependent decrease in ubiquitin signal in perinuclear aggregate bodies, SKOV3 cells were pretreated with

either DMSO or 200 nM bortezomib for 24 hours and then treatment was followed with a dose-response of TAK-243 (Figure 13). These cells were then fixed for immunofluorescence at 0, 1, 2, 4, 6, 24 hours after TAK-243 treatment and stained for K48 ubiquitin linkages and p62. In these studies, perinuclear aggregate-associated p62 staining was observed only in the cells pre-treated with 200 nM bortezomib for 24 hours. K48-linked ubiquitin chain signal increased in the bortezomib pre-treated cells and then cytosolic signal of K48-linked ubiquitin chains was suppressed by treatment of TAK-243. However, K48-linked ubiquitin chain signal seemed unaffected out to 24 hours in the perinuclear bodies, where the signal colocalized with p62 and there were no examples of perinuclear bodies that stained positive for p62 but did not have K48 ubiquitin staining (Figure 14). Looking at longer timepoints was limited by the cytotoxicity of the long exposure to bortezomib.

Mass Spectrometry

A subset of samples was selected for ubiquitin linkage quantification by mass spectrometry. These samples were whole cell extracts of SKOV3 cells either pre-treated with bortezomib for 24 hours or incubated with DMSO then treated with DMSO, TAK-243, or bortezomib for 0 or 6 hours. Peptides were identified and quantified for 5 out of 7 linkage sites including K6, K11, K27, K48, and K63 (Table 1a). These peptides contain a lysine with a branch of the GlyGly remnant from the connected ubiquitin's C-terminus. Figures containing the complete quantification results can be found in the appendix (Figure 15).

Quantification results were highly consistent with total ubiquitin immunoblot results (Figure 10). While there were stark differences in the relative amounts of each linkage there did not appear to be any difference in the response to bortezomib and TAK-243. There were two

samples that did not have any detectable K6 linkage peptide and one sample that did not have any detectable K27 linkage peptide. All of which were in samples treated with TAK-243 that saw a decrease in all ubiquitin linkages. This likely indicates these linkages were below detectable limits. The majority of ubiquitin linkages found were K48 linkages followed by K63. K6, K11, and K27 linkages made up a small minority of the ubiquitin linkages detected. Despite this, all of the linkages accumulated in response to bortezomib treatment and all linkages decreased in response to TAK-243. In the sample that was first treated with bortezomib and then treated with TAK-243, the ubiquitin linkages for all types returned to the baseline of the DMSO-treated sample.

This result is potentially in conflict with published results from Kim et al. in which a different method was used to quantify changes in ubiquitin linkage types in response to bortezomib treatment (Kim et al,, 2011). These scientists used a selective antibody that recognizes the diGly remnant peptide of ubiquitin conjugates digested with protease to isolate ubiquitin conjugates from stable isotope labeled HCT116 and 293T cell lysates. Using this method, it was observed that diGly peptides corresponding to K6, K11, K27, K33, and K48 increased by about 2-fold after 2 hours of treatment with bortezomib, while peptides corresponding to K63 ubiquitin conjugates did not increase throughout a timecourse of bortezomib treatment (Kim et al., 2011). A number of experimental differences can introduce variables consistent with these results; particularly the use of a diGly antibody to isolate conjugates before digestion but also different cell types, timepoints and doses of bortezomib that could have temporal differences in response. Further study is required to determine the significance of these differences.

Chapter IV

Discussion

Significance of Results

The aim of this research was to identify if there was a population of ubiquitin conjugates that are resistant to deubiquitinases following treatment with bortezomib and if this population is associated with nuclear-adjacent aggresomal bodies. We have shown data that demonstrates that there is a sub-population of ubiquitinated conjugates that form in response to treatment with bortezomib and aggregate adjacent to the nucleus. We have also demonstrated that ubiquitin conjugates found in this body are not deubiquitinated or destroyed following TAK-243 treatment, unlike the bulk of ubiquitin conjugates found elsewhere in the cell. We have shown that these bodies stain positive for K48-linked ubiquitin chains but were unable to demonstrate the presence or absence of other ubiquitin linkage types in these bodies due to reage nt limitations. We have also shown that these bodies colocalize with p62, a marker of aggresomes, as well as a dye that binds to aggregated proteins. These data suggest that ubiquitinated conjugates accumulate following inhibition of the proteasome and that these conjugates aggregate together into inclusion bodies that isolate them from methods of ubiquitin-conjugate clearance that are highlighted by inhibition of UAE with TAK-243, such as deubiquitinases or autophagy. Furthermore, there does not appear to be any particular preference for a particular subset of the five ubiquitin linkage types measured by mass spectrometry.

SKOV3 and HCT116 human cancer cell lines were utilized for experiments to address this hypothesis. Immunoblotting and immunofluorescence were utilized to assay levels and

localization of ubiquitin conjugate populations in response to treatment with bortezomib and TAK-243. Inhibition of the proteasome with bortezomib causes total ubiquitin conjugates to shift from the nucleus to the cytoplasm as well as an increase in K48-linked ubiquitin conjugates throughout the cell. Efforts to look at K63-linked ubiquitin chain population levels and localization were unsuccessful. Over longer treatment periods, a 24 hour treatment was used here, ubiquitin conjugates can be seen aggregating in inclusion bodies adjacent to the nucleus. For the purposes of this study, these bodies will be referred to as aggresomes. An effort was made to discern which ubiquitin linkages were found in these bodies but we were unable to determine as we were only able to follow K48-ubiquitin and total polyubiquitin in cellular localization studies. These ubiquitin-positive inclusion bodies colocalized with markers of aggresome formation such as P62 and NBR1 as well as a dye that binds to aggregated protein. This result suggests that these inclusion bodies are likely aggresomes.

Treatment with TAK-243 causes a rapid decrease in total ubiquitin conjugate levels throughout the cell. In cells treated with bortezomib for shorter periods, say less than 6 hours, which have a large broad increase in both total ubiquitin conjugate and K48-specific ubiquitin staining; TAK-243 treatment for 1 hour is enough to reduce polyubiquitin levels back to baseline. However, if bortezomib-induced aggresomes were allowed to form, treatment with TAK-243 had no effect on ubiquitin conjugate levels inside the aggresome. One explanation for this result could be that the rate of clearance of ubiquitin chains in these compartments is slower than in the rest of the cell. However, incubations of TAK-243 for up to 24 hours did not lead to any more turnover of these ubiquitin chains.

To support these cellular localization studies, a small amount of lysate from the bortezomib and TAK-243 treated SKOV3 cells was set aside for mass spectrometry. Lysate

from WSU cells that had been grown in stable isotope labelled media was added to each sample as an internal control to allow comparison across samples. Peptides were identified and quantified for seven linkage sites including K6, K11, K27, K48, K63. TAK-243 decreased the levels of K48-linked ubiquitin by five fold over the six hour treatment. Likewise, a 24 hour bortezomib treatment increased the levels of K48-linked ubiquitin by over six fold. K48-linked ubiquitin levels returned to untreated levels when bortezomib treatment was followed by TAK-243. This data correlates well with what was observed by immunofluorescence and immunoblot. A similar trend was observed for all of the measured ubiquitin linkage types. In all cases, bortezomib followed by TAK-243 treatment reduced ubiquitin linked proteins to untreated levels but not to levels reached with TAK-243 treatment alone.

One interpretation of this data is that inhibiting proteasome causes ubiquitin-conjugated proteins, no longer being degraded at full capacity, to begin accumulating faster than other mechanisms of protein clearance can handle. Meanwhile, the UAE pathway is continuing to add ubiquitin molecules to conjugates and misfolded or unwanted proteins faster than deubiquitinases or other protein clearance processes can remove them. We know that proteasome inhibition can activate the UPR pathway and overwhelm processes for protein clearance, leading to sequestration into protective compartments, such as JUNQ, and/or destined for clearance through bulk degradative pathways, such as macroautophagy. The data is consistent with this interpretation but is not sufficient to prove it.

Study Limitations

One aim of this study was to demonstrate the presence of a DUB-resistant ubiquitin conjugate population. When UAE is inhibited with TAK-243, a rapid loss of ubiquitin

conjugates is observed (Hyer et al., 2018). It is believed that this is primarily driven by a shift in the equilibrium of ubiquitin conjugation/deconjugation (Brownell, 2010). It is also believed that a reverse dynamic is involved with proteasome inhibition, where conjugates accumulate faster than they can be deconjugated. While the observations in this study are consistent with this hypothesis, alternative explanations have not been ruled out by the experiments performed. One way to address this question would be to extract the inclusion bodies containing ubiquitin conjugates that remain after TAK-243 treatment and use them as substrate for DUB activity to see if they are completely protected or just degraded more slowly. However, a method for this experiment was not developed in time.

Another aim of this study was to demonstrate a differential in the dynamics of loss of ubiquitin-conjugate population pool in different ubiquitin linkage types. A K48-specific antibody was well characterized for use in both immunofluorescence and western blot but conditions for other commercially available linkage-specific reagents did not work. As such, we were only able to track K48-linked ubiquitin and total polyubiquitin in cell localization assays by immunofluorescence and the mass spectrometry result suggests that a large portion of the total polyubiquitin observed is K48-linked. This means we cannot draw any conclusions about cell localization of other polyubiquitin linkage types.

Additionally, the experiments performed do not rule out that K48-ubiquitin conjugates are slowly being incorporated into perinuclear aggresomal bodies as opposed to being deconjugated by DUBs. To better demonstrate the fate of the conjugates as they decrease in the cytoplasm would need a method to eliminate incorporation into the perinuclear bodies and/or inhibition of DUB activity. Utilization of a functional DUB inhibitor, such as ubiquitin-vinylsulfone, could be used as a probe to address the requirement of DUB activity in K48-

polyubiquitin deconjugation in an *ex vivo* cell lysate experiment. This experiment in combination with an experiment demonstrating a requirement for p62 in the sequestration of ubiquitinated proteins into perinuclear bodies, as recently performed by Sha et al., might address this limitation.

Direction of Future Research

Recent work by Zhe Sha et al. shows an increased sensitivity to bortezomib in autophagy deficient cells suggesting a role for autophagy in resolving built up ubiquitin conjugates. In this work, Sha demonstrates a requirement for p62 in the sequestration of ubiquitinated proteins into perinuclear bodies (Sha et al., 2018). This result correlates with results shown here and points to future work in further characterizing compensation mechanisms of cells in response to proteasome inhibition.

Additional studies should aim to characterize the aggregated bodies that accumulate with proteasome inhibition using markers of autophagy, the unfolded protein response, and JUNQ or IPOD quality-control inclusion bodies. A better understanding of their formation and resolution would benefit this characterization. Using colocalization immunofluorescence assays looking at markers such as LC3, HDAC6, and NBR1 or looking by western blot at markers of proteotoxic stress such as activated ATF6, PERK, and IRE1 over a time-course of proteasome pre-treatment then followed by addition of TAK-243 to see the fate of ubiquitin conjugate resolution would help to elucidate what the role of these bodies may be.

One set of experiments that would expand on these results would be to look at DUB activity using the ubiquitin conjugates found in these nuclear adjacent bodies as a substrate. If we were to take lysates of cells treated with TAK-243 or bortezomib followed by TAK-243 and

extract bulk ubiquitin conjugates to use as substrates for a DUB activity assay it might help to answer if this population were DUB resistent or just sequestered. Development of assay conditions for other ubiquitin-linkage specific reagents would further support the interpretation that the aggresomal bodies are of different linkage types in response to proteasome and UAE inhibition.

Conclusions

I hypothesized that there was a differential in a subpopulation of ubiquitin conjugate dynamics in response to proteasome inhibition. Data from colocalization immunofluorescence studies showed the formation of aggresomal bodies in response to prolonged bortezomib treatment that contained a population of ubiquitin conjugates that were differentially affected by treatment with TAK-243. Assays to monitor linkage-specific ubiquitin chains other than K48, the most abundant linkage type, were not identified but quantitative measurement of several linkage types indicates no differential in response in overall conjugate levels in response to bortezomib/TAK-243 treatment. Together this data suggests that ubiquitin conjugates, regardless of linkage type, accumulate in response to bortezomib and aggregate in inclusion bodies, which appear primarily to be nuclear adjacent. Here, they are protected from deubiquitination; unlike ubiquitin-conjugates found in the cytoplasm and nucleus.

Appendix

a)

			SKOV3		WSU K8; R10
Site	**Sequence**	**charge**	**m/z**	**RT**	**m/z**
K6	_MQIFVK(GlyGly)TLTGK_	3	460.5954	52.53	465.9382
K6	_M(ox)QIFVK(GlyGly)TLTGK_	3	465.9270	42.74	471.2698
K11	_TLTGK(GlyGly)TITLEVEPSDTIENVK_	3	801.4269	59.70	806.7697
K27	_TITLEVEPSDTIENVK(GlyGly)AK_	2	1051.0548	54.98	1059.06906
K29	_TITLEVEPSDTIENVKAK(GlyGly)_	3	701.0390	55.26	706.3818
K27&29	_TITLEVEPSDTIENVK(GlyGly)AK(GlyGly)IQDK_	4	675.6079	67.10	681.618595
K29	_AK(GlyGly)IQDKEGIPPDQQR_	4	459.9945	21.11	466.5037
K29	_AK(GlyGly)IQDKEGIPPDQQR_	3	612.9903	21.13	621.6692
K33	_IQDK(GlyGly)EGIPPDQQR_	3	546.6129	20.32	552.6204
K48	_LIFAGK(GlyGly)QLEDGR_	3	487.6001	43.71	493.6075
K48	_LIFAGK(GlyGly)QLEDGR_	2	730.8964	43.73	739.9077
K63	_TLSDYNIQK(GlyGly)ESTLHLVLR_	3	748.7376	59.21	754.7451
K63	_TLSDYNIQK(GlyGly)ESTLHLVLR_	4	561.8050	58.97	566.3106

b)

Raw Intensity							
Linkage site	**Sample**	**DMSO**	**TAK-243 (6hr)**	**bortezomib (24 hr) DMSO (6hr)**	**bortezomib (24hr)**	**bortezomib (24 hr) TAK-243 (6hr)**	**bortezomib (6hr)**
K6	**SKOV3**	22,052	*LOD*	338,277	70,394	*LOD*	156,214
	WSU	162,835	185,514	170,051	67,714	72,475	197,183
K11	**SKOV3**	598,715	98,589	2,333,519	855,150	106,716	1,078,666
	WSU	1,173,176	1,442,378	1,081,326	884,524	657,576	1,328,350
K27	**SKOV3**	47,078	*LOD*	901,422	317,717	27,975	223,924
	WSU	314,100	317,839	248,959	193,734	162,330	354,310
K48	**SKOV3**	15,630,399	2,415,020	93,052,441	38,913,306	9,409,633	42,072,969
	WSU	47,226,189	37,122,621	42,868,338	36,551,371	23,826,097	48,663,581
K63	**SKOV3**	4,041,553	917,115	15,698,554	5,966,170	1,015,614	4,320,611
	WSU	5,437,934	6,060,389	4,878,278	3,715,095	2,256,595	5,071,094

c)

Normalized Intensity (SKOV3/WSU)						
Linkage site	**DMSO**	**TAK-243 (6hr)**	**bortezomib (24 hr) DMSO (6hr)**	**bortezomib (24hr)**	**bortezomib (24 hr) TAK-243 (6hr)**	**bortezomib (6hr)**
K6	**0.1**	**--**	**2.0**	**1.0**	**--**	**0.8**
K11	**0.5**	**0.1**	**2.2**	**1.0**	**0.2**	**0.8**
K27	**0.2**	**--**	**3.6**	**1.6**	**0.2**	**0.6**
K48	**0.3**	**0.1**	**2.2**	**1.1**	**0.4**	**0.9**
K63	**0.7**	**0.2**	**3.2**	**1.6**	**0.5**	**0.9**

d)

Relative Amount (RA of N = $(DMSO_{WSU}/N_{WSU})*N_{SKOV3}$)						
Linkage site	**DMSO**	**TAK-243 (6hr)**	**bortezomib (24 hr) DMSO (6hr)**	**bortezomib (24hr)**	**bortezomib (24 hr) TAK-243 (6hr)**	**bortezomib (6hr)**
K6	**22052.0**	**--**	**323922.4**	**169279.7**	**--**	**129002.5**
K11	**598715.0**	**80188.6**	**2531732.8**	**1134216.2**	**190391.1**	**952659.4**
K27	**47078.0**	**--**	**1137282.2**	**515113.0**	**54130.2**	**198511.3**
K48	**15630399.0**	**3072309.8**	**102511839.1**	**50277926.5**	**18651024.0**	**40830246.0**
K63	**4041553.0**	**822919.3**	**17499556.3**	**8732923.0**	**2447422.7**	**4633161.5**

Table 1. Relative amount of ubiquitin linkage types in SKOV3 cells treated with bortezomib and/or TAK-243. Total cellular proteins were resolved by SDS-PAGE. Gel bands above 25 kDa were sliced from the gel and an in-gel digestion was performed using a combination of proteases, Lys-C and Trypsin. Each sample was analyzed on an Orbitrap-Fusion Mass Spectrometer over a 120 minute gradient in targeted MS2 mode focusing on diGly-peptides from each Ubiquitin linkage site. a) Unique peptide map of ubiquitin-linkage types observed in cells treated with bortezomib and/or TAK-243. Successfully identified and quantified 5 out of 7 linkage sites including K6, K11, K27, K48, and K63. b) raw MS data were processed using the combination of MaxQuant and Mascot. c) To obtain the normalized intensity of each ubiquitin linkage type, the ratio of raw intensity of heavy-labeled WSU lysate and light-labeled SKOV3 lysate was measured for the peptide indicating each linkage type. The observed molecular weight in the heavy-labeled WSU lysate is 2 Da greater per lysine and arginine residue than expected due to the heavy-isotope labeling. d) To get a more representative value of the relative levels of each linkage across samples, the normalized intensity was then multiplied by the ratio of the WSU lysate from the DMSO control over the WSU lysate corresponding to the sample in question (Relative Amount of N = $(DMSO_{WSU}/N_{WSU})*N_{SKOV3}$). This value represents the relative amount of each linkage type observed in each sample. LOD = signal below limit of detection.

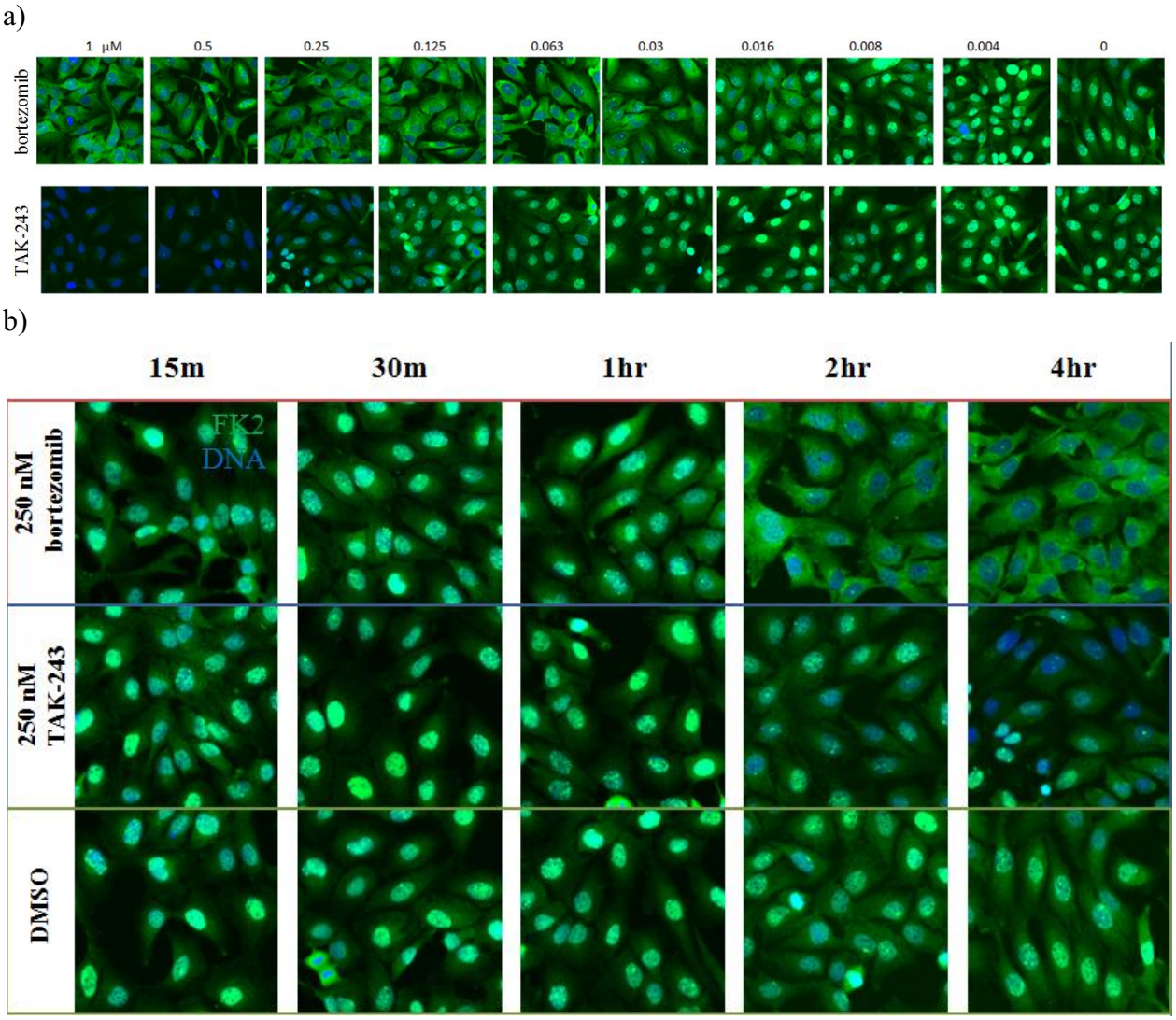

Figure 6. Total ubiquitin conjugate levels of SKOV3 cells treated with a dose response of TAK-243 for 15 minutes, 30 minutes, 1 hour, 2 hours, or 4 hours. Total ubiquitin levels were measured by immunofluorescent staining of a polyubiquitin antibody (FK2; green). DNA was stained with Hoechst Dye (blue). a. Dose-response data shown for 4 hour treatment. b. Time-course data shown for 250 nM dose.

a)

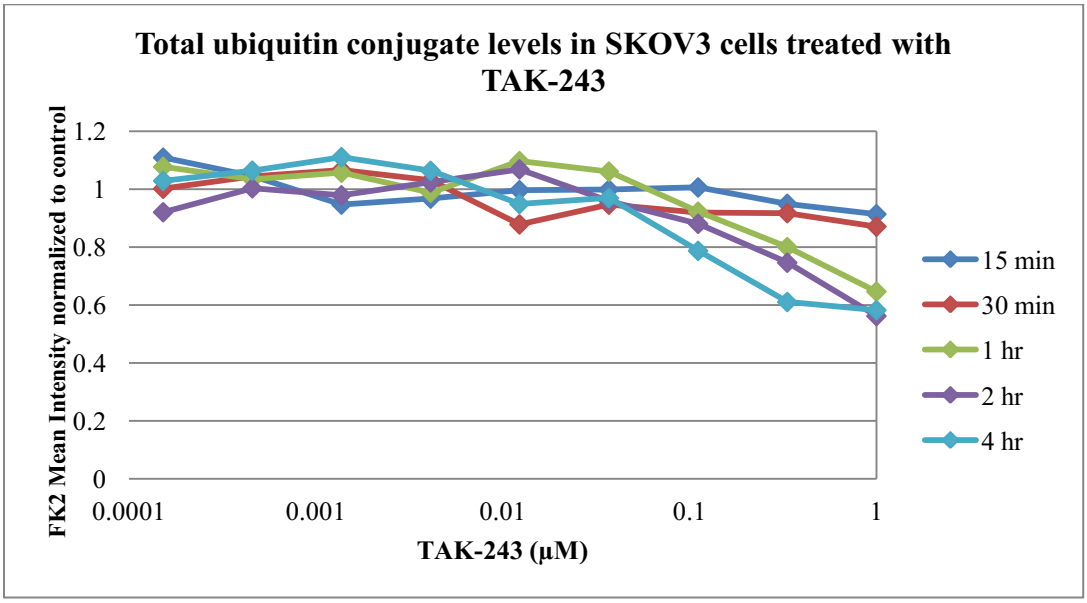

b)

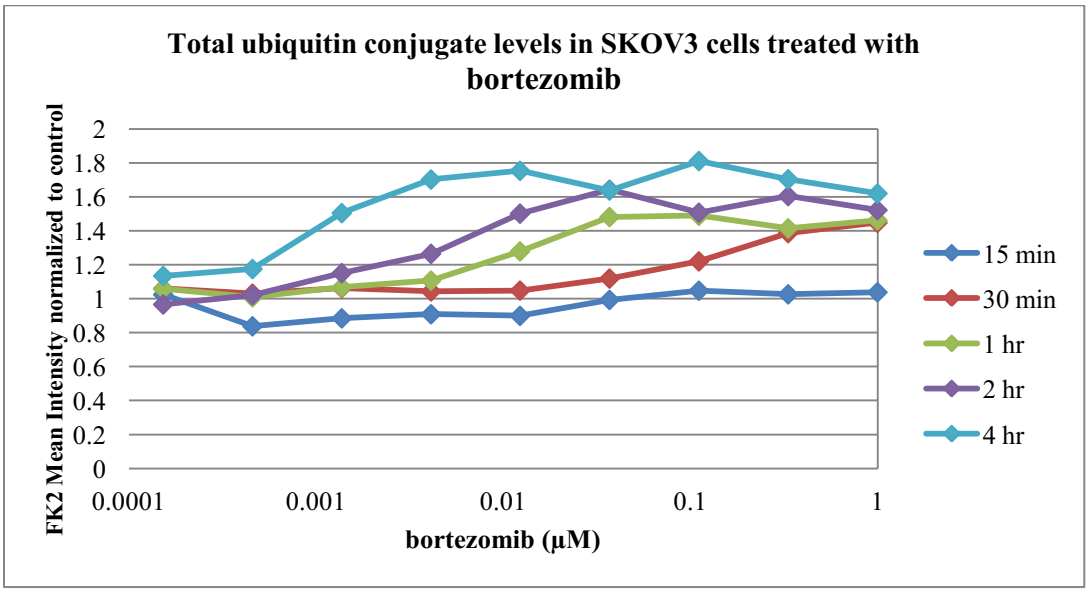

Figure 7. Quantitation and normalization of total ubiquitin conjugate levels of SKOV3 cells treated with bortezomib or TAK-243. Average cell intensity was measured for SKOV3 cells (shown in Figure 6) treated with a) TAK-243 or b) bortezomib, stained for total polyubiquitin, and normalized to untreated control.

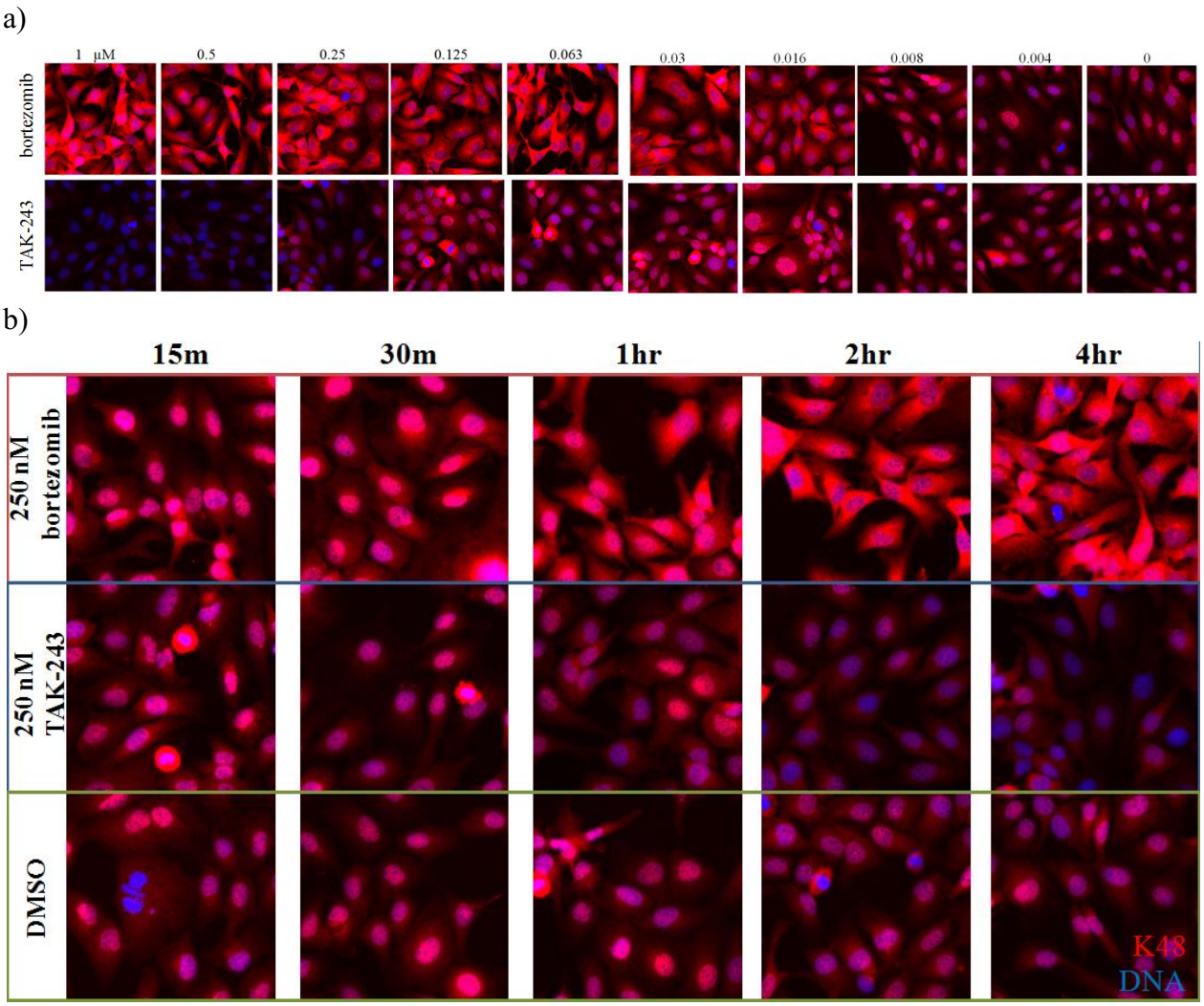

Figure 8. K48-ubiquitin conjugate levels of SKOV3 cells treated with a dose response of TAK-243 for 15 minutes, 30 minutes, 1 hour, 2 hours, or 4 hours. Total ubiquitin levels were measured by immunofluorescent staining of a K48 linkage specific antibody (K48; red). DNA was stained with Hoechst Dye (blue). a) Dose-response data shown for 4 hour treatment. b) Time-course data shown for 250 nM dose.

a)

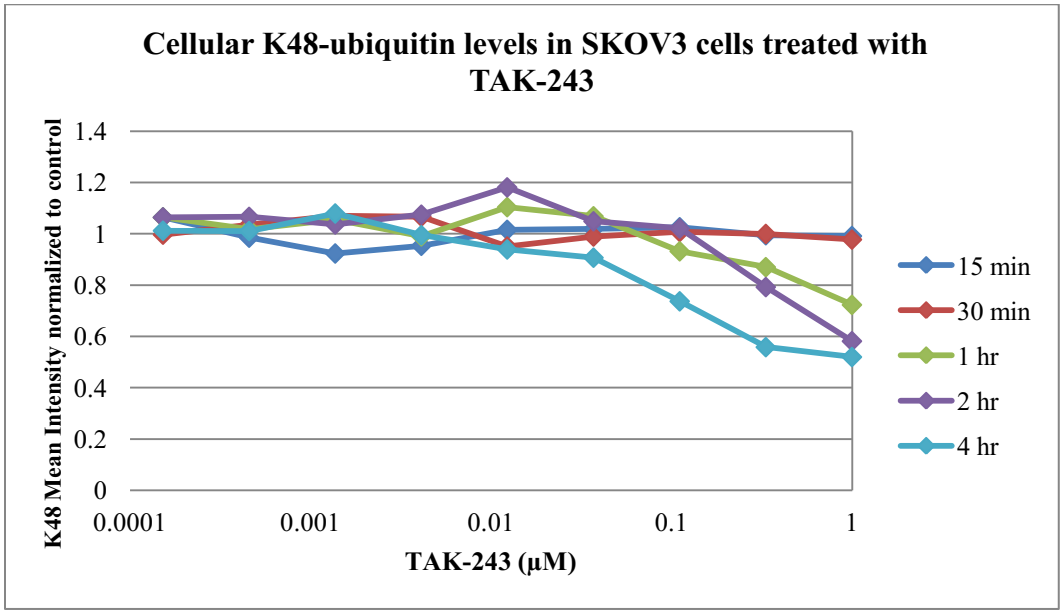

b)

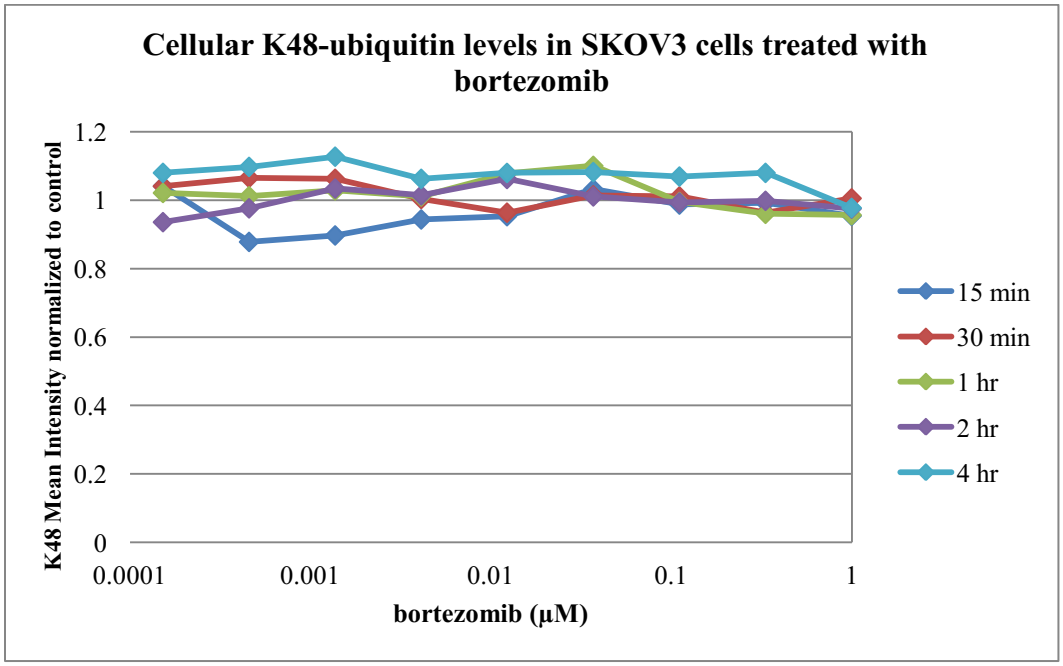

Figure 9. Quantitation and normalization of K48- ubiquitin conjugate levels of SKOV3 cells treated with bortezomib or TAK-243. Average cell intensity was measured for SKOV3 cells (shown in Figure 8) treated with a) TAK-243 or b) bortezomib, stained for K48-linked ubiquitin, and normalized to untreated control.

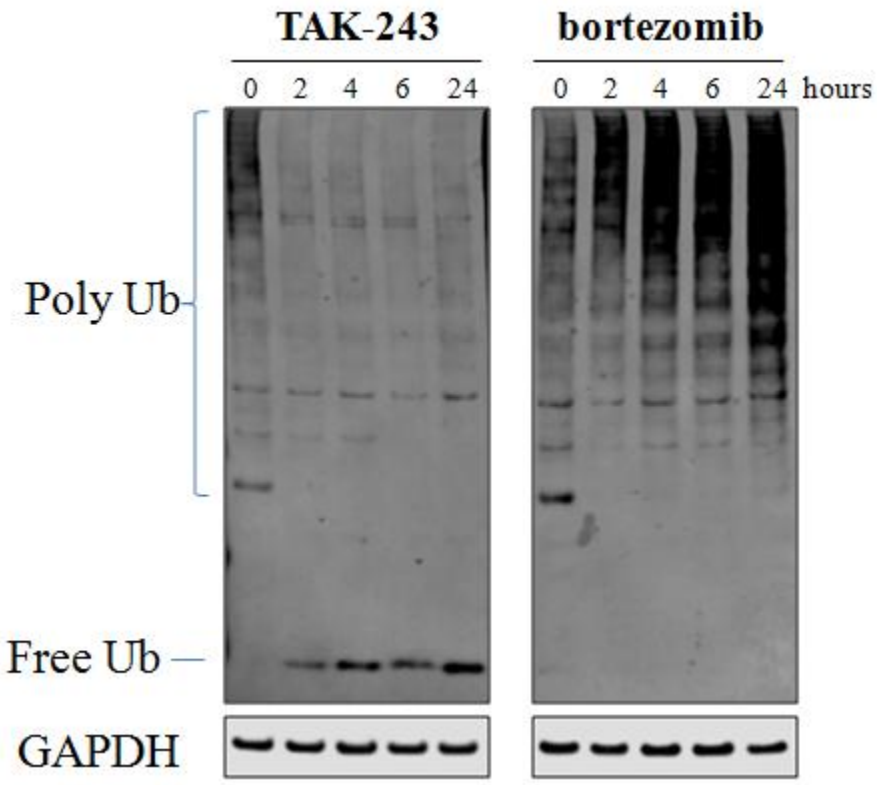

Figure 10. Western blot analysis of SKOV3 cells treated with 0.5 µM of TAK-243 or 0.5µM bortezomib for 0, 2, 4, 6, or 24 hours. Time dependent modulation of total ubiquitin was observed with both treatments. Free ubiquitin observed within 2 hours of treatment with TAK-243 indicating deconjugation from substrate proteins. GAPDH included as a loading control.

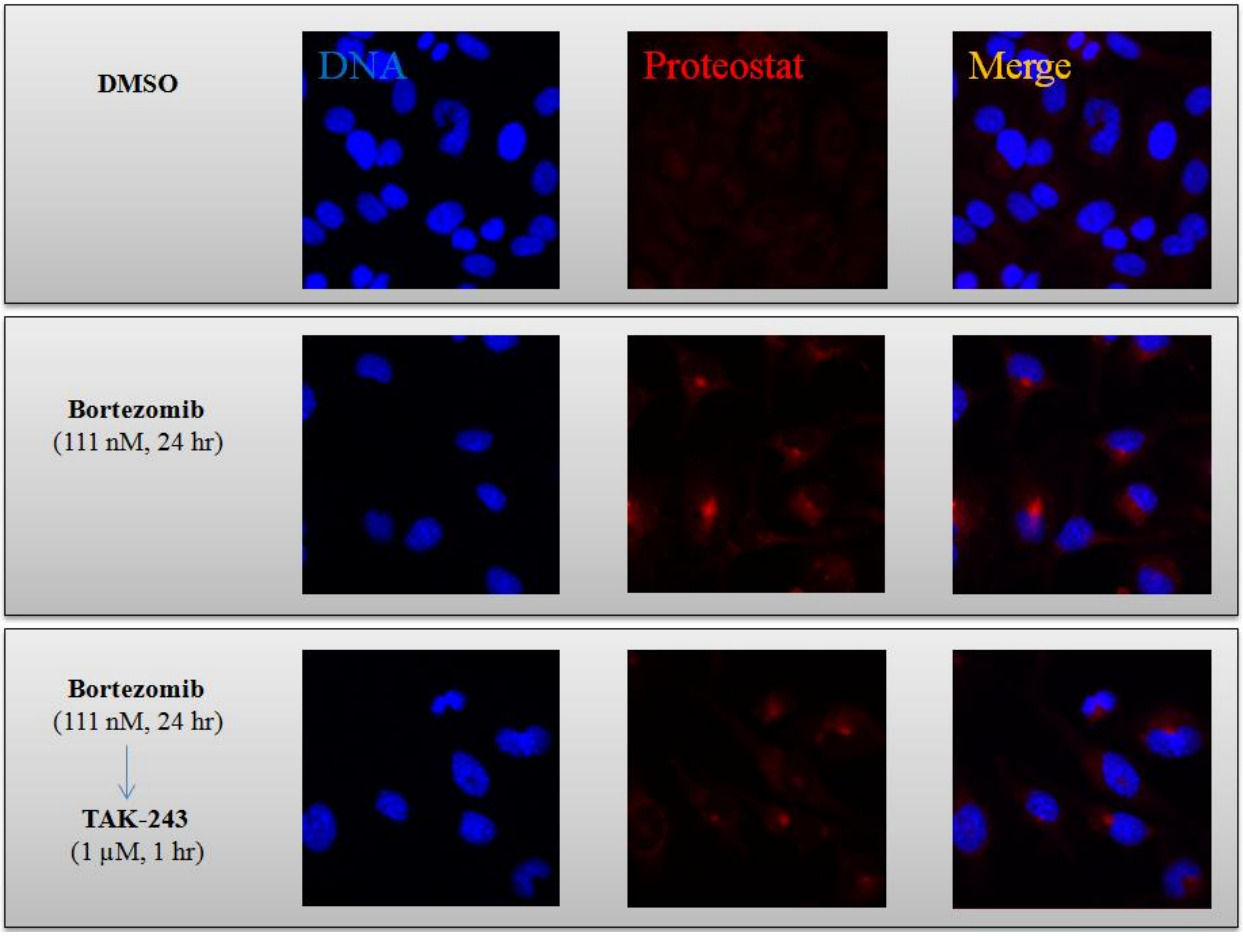

Figure 11. Bortezomib induces perinuclear aggregate formation which TAK-243 does not appear to modulate. SKOV3cells pretreated with 111 nM bortezomib for 24 hours followed by 1 µM of TAK-243 treatment for 1 hour. DNA stained with Hoechst dye (blue) and proteostat dye (ENZO; red), which binds non-specifically to aggregated proteins.

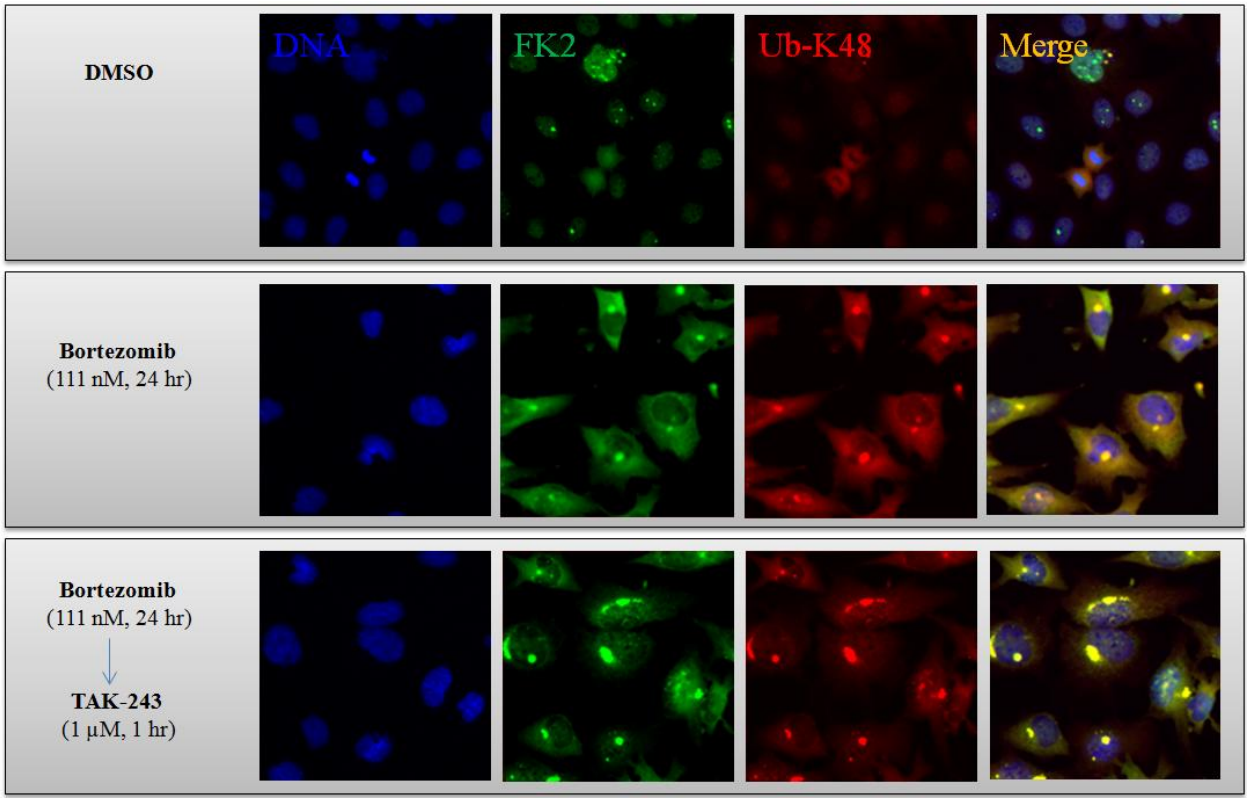

Figure 12. Ubiquitin conjugates in perinuclear aggregate inclusion bodies are not reduced by TAK-243 treatment. SKOV3cells pretreated with 111 nM bortezomib for 24 hours followed by 1 μM of TAK-243 treatment for 1 hour. DNA stained with Hoescht (blue), total polyubiquitin (green), and K48-linked polyubiquitin (red).

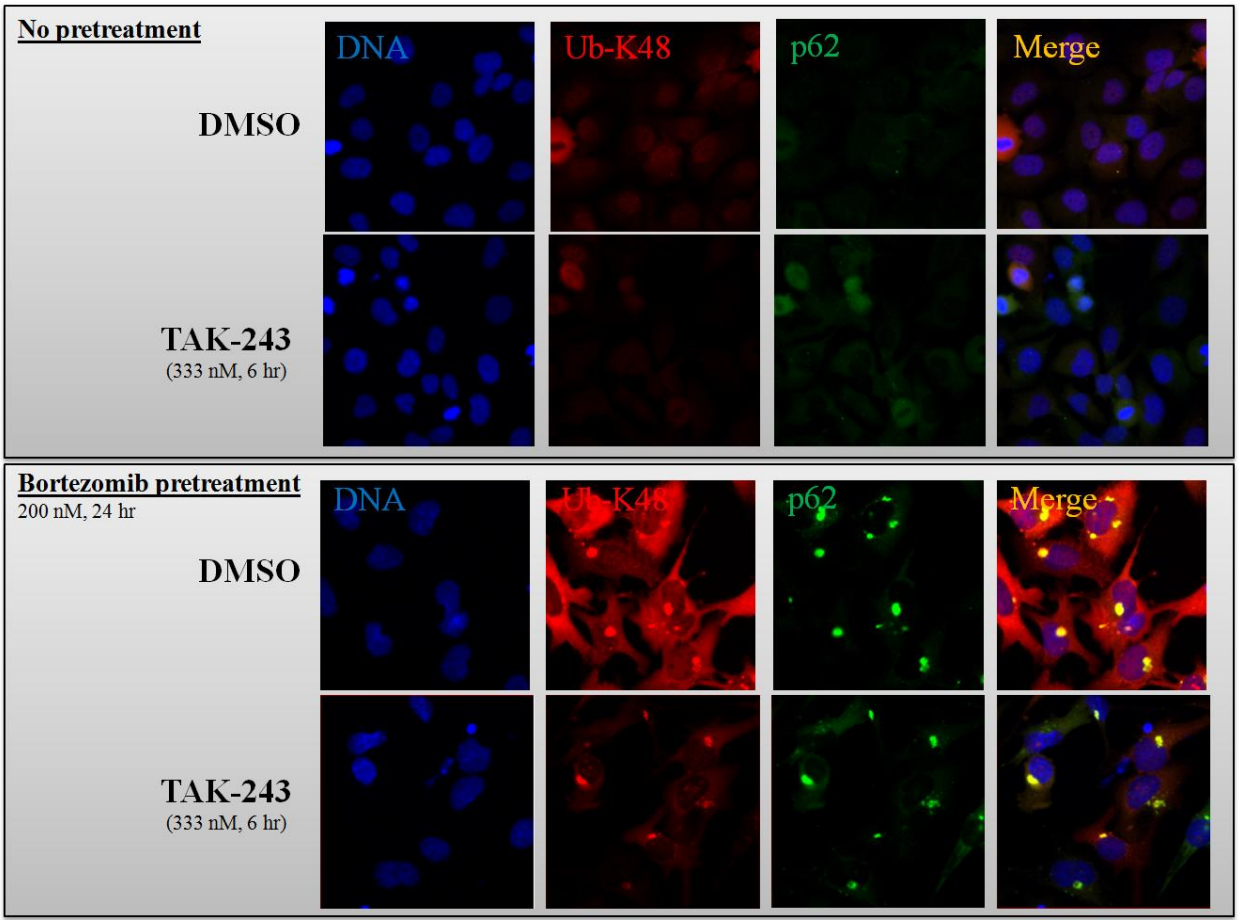

Figure 13. Strong, diffuse Ub-K48 signal is observed with bortezomib treatment alone that decreases when cells are subsequently treated with TAK-243 for 6 hours. K48 (red) staining that overlaps with p62 (green) remains when cells are then treated with TAK-243. SKOV3cells pretreated with 200 nM bortezomib or DMSO for 24 hours followed by 333 nM of TAK-243or DMSO treatment for 6 hours. DNA stained with Hoescht (blue).

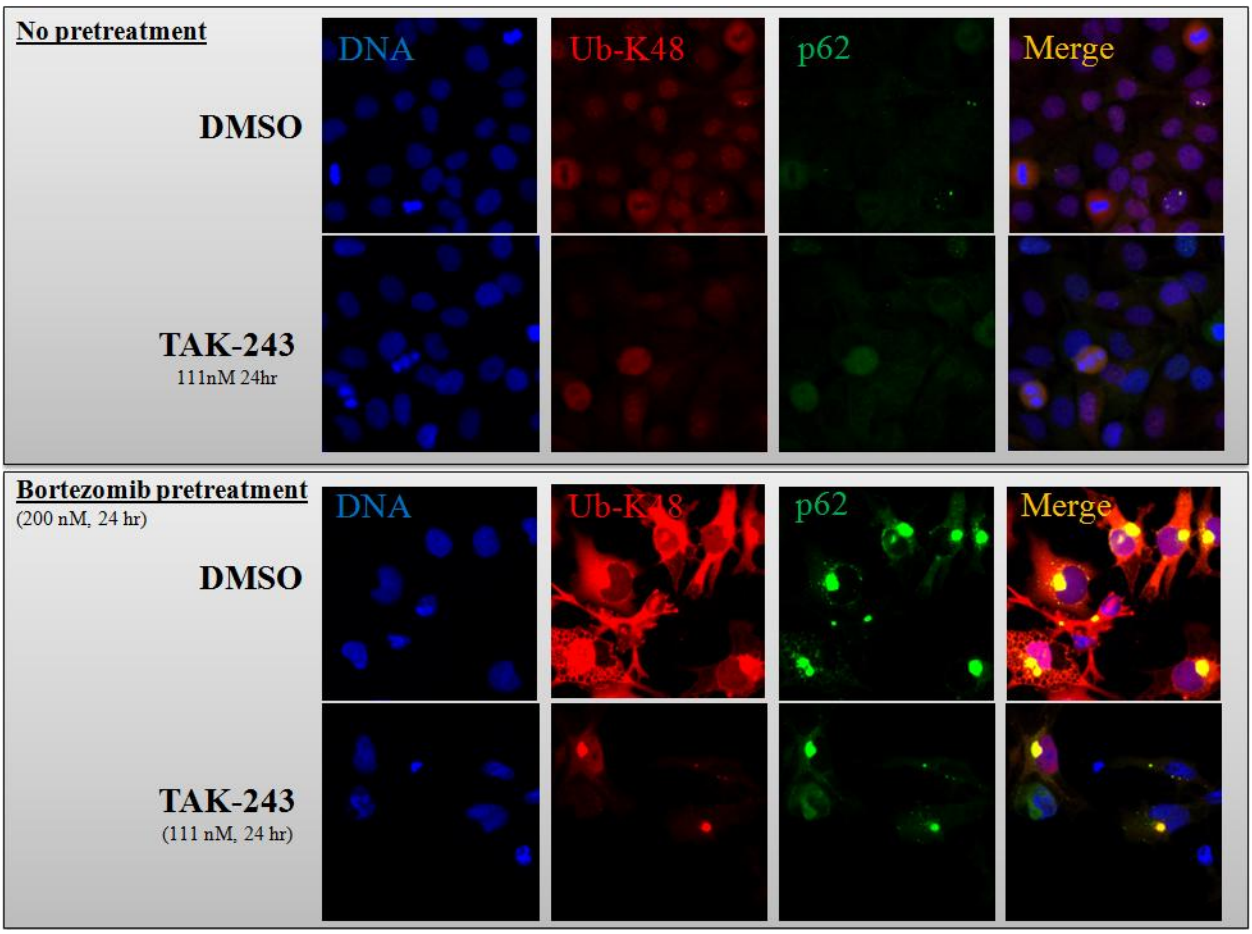

Figure 14. Strong, diffuse Ub-K48 signal is observed with bortezomib treatment alone that decreases when cells are subsequently treated with TAK-243 for 24 hours. K48 (red) staining that overlaps with p62 (green) remains when cells are then treated with TAK-243, even when treated for 24 hours. SKOV3cells pretreated with 200 nM bortezomib or DMSO for 24 hours followed by 333 nM of TAK-243or DMSO treatment for 24 hours. Longer timepoints were not feasible due to widespread cell death. DNA stained with Hoescht (blue).

a)

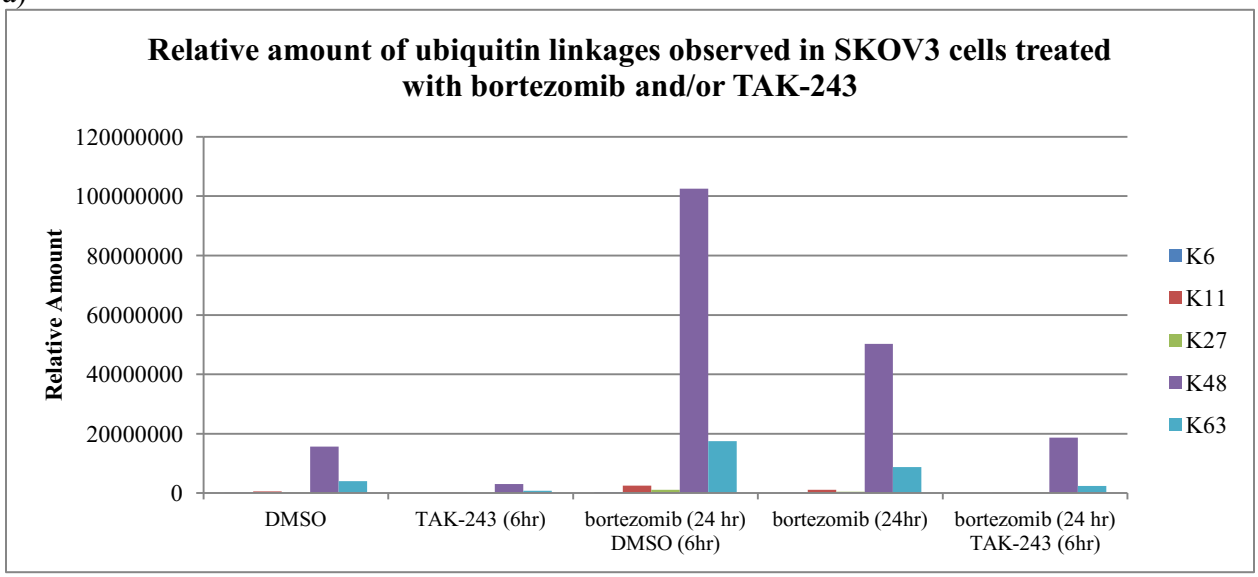

b)

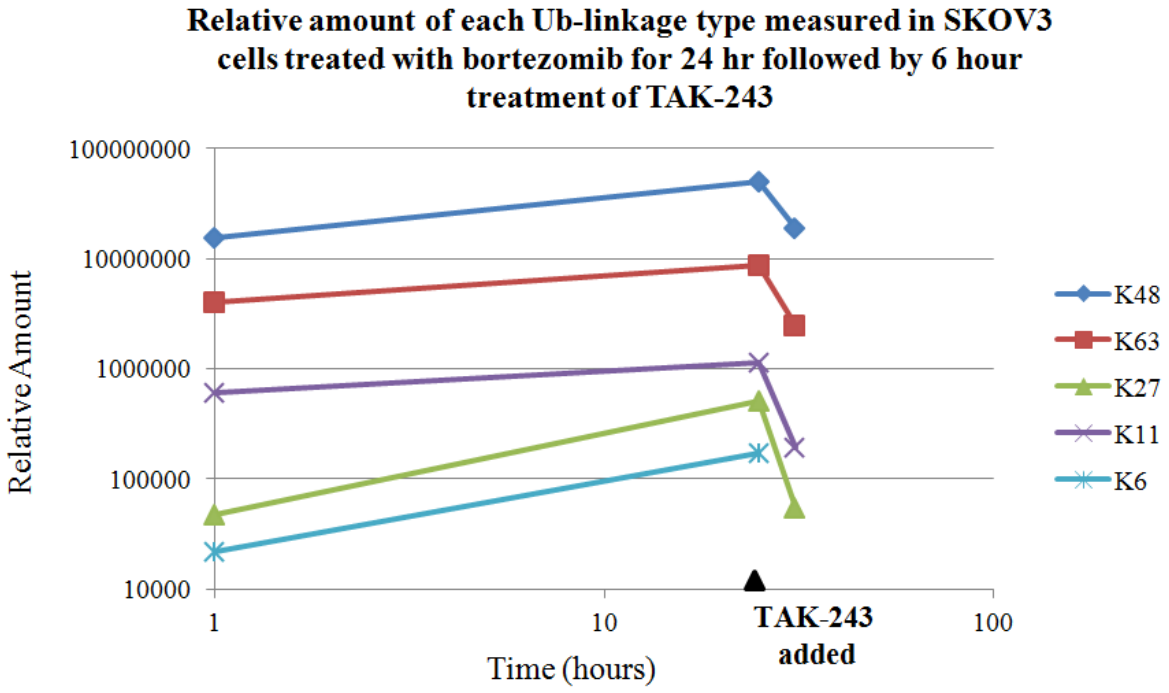

Figure 15. Relative amounts of ubiquitin linkages observed in SKOV3cells pretreated with bortezomib and/or TAK-243 as measured by mass spectrometry. Western blot data of these samples can be found in Figure 10 a) Relative amounts of each ubiquitin linkage type b) Relative amounts of each ubiquitin linkage type over time represented in log scale.

References

Beckwith, R., Estrin, E., Worden, E. J., & Martin, A. (2013). Reconstitution of the 26S proteasome reveals functional asymmetries in its AAA+ unfoldase. *Nat Struct Mol Biol*, 20(10), 1164-1172.

Bedford, L., Lowe, J., Dick, L. R., & Brownell, J. E. (2011). Ubiquitin-like protein conjugation and the ubiquitin-proteasome system as drug targets. *Nat Rev Drug Discov.*, 10(1):29-46.

Blackburn, C., Gigstad, K. M., Hales, P., Garcia, K., Jones, M., Bruzzese, F. J., Barrett, C., Liu, J. X., Soucy, T. A., Sappal, D. S., Bump, N., Olhava, E. J., Fleming, P., Dick, L. R., Tsu, C., Sintchak, M. D., Blank, J. L. (2010). Characterization of a new series of non-covalent proteasome inhibitors with exquisite potency and selectivity for the 20S β5-subunit. *Biochem. J.,* 430, 461-476.

Brownell, J. E., Sintchak, M. D., Gavin, J. M., Liao, H., Bruzzese, F. J., Bump, N. J., Soucy, T. A., Milhollen, M. A., Yang, X., Burkhardt, A. L., Ma, J., Loke, H. K., Lingaraj, T., Wu, D., Hamman, K. B., Spelman, J. J., Cullis, C. A., Langston, S. P., Vyskocil, S., Sells, T. B., Mallender, W. D., Visiers, I., Li, P., Claiborne, C. F., Rolfe, M., Bolen, J. B., & Dick, L. R. (2010). Substrate-assisted inhibition of ubiquitin-like protein-activating enzymes: the NEDD8 E1 inhibitor MLN4924 forms a NEDD8-AMP mimetic in situ. *Mol Cell,* 37(1), 102-111.

Chen, L., Brewer, M. D., Guo, L., Wang, R., Jiang, P., & Yang, X. (2017). Enhanced degradation of misfolded proteins promotes tumorigenisis. *Cell Reports,* 18, 3143-3154.

Chen, S., Blank, J. L., Peters, T., Liu, T. P., Rappoli, D. M., Pickard, M. D., Menon, S., Yu, J., Driscoll, D. L., Lingaraj, T., Burkhardt, A. L., Chen, W., Garcia, K., Sappal, D. S., Gray, J., Hales, P., Leroy, P. J., Ringeling, J., Rabino, C., Spelman, J. J., Morgenstern, J. P., & Lightcap, E. S. (2010). Genome-wide siRNA screen for modulators of cell death induced by proteasome inhibitor bortezomib. *Cancer Res,* 70(10), 4318-4326.

Cottini F. et al. (2014). Resistance to Proteasome Inhibitors in Multiple Myeloma. In: Dou Q. (eds) Resistance to Proeasome Inhibition in Cancer. Resistance to Targeted Anti-Cancer Therapeutics. Springer, Cham. Pp 47-80.

Deshaies, R. (2014). Proteotoxic crisis, the ubiquitin-proteasome system, and cancer therapy. *BMC Biol., 12(94).*

Driscoll, J.J. & DeChowdhury, R. (2010). Therapeutically targeting the SUMOylation, Ubiquitination and Proteasome pathways as a novel anticancer strategy. *Targ Oncol.*, 5(4), 281-289.

Goldberg, A. L. (2012). Development of proteasome inhibitors as research tools and cancer drugs. *J Cell Biol.*, 199(4), 583-588.

Haas, A. L., Warms, J. V., Hershko, A., & Rose, I. A. (1982). Ubiquitin-activating enzyme. Mechanism and role in protein-ubiquitin conjugation. *J Biol Chem*, 257(5), 2543-2548.

Haglund, K., Di Fiore, P. P. & Dikic, I. (2003). Distinct monoubiquitin signals in receptor endocytosis. *Trends Biochem Sci.,* 28, 598–603.

Hanahan, D. & Weinberg, R. A. (2011). Hallmarks of Cancer: The Next Generation. *Cell,* 144(5), 646-674.

Hyer, M. L., Milhollen, M. A., Ciavarri, J., Fleming, P., Traore, T., Sappal, D., Huck, J., Shi, J., Gavin, J., Brownell, J., Yang, Y., Stringer, B., Griffin, R., Bruzzese, F., Soucy, T., Duffy, J., Rabino, C., Riceberg, J., Hoar, K., Lublinsky, A., Menon, S., Sintchak, M., Bump, N., Pulukui, S., Langston, S., Tirrell, S., Kuranda, M., Veiby, P., Newcomb, J., Li, P., Wu, J. T., Powe, J., Dick, L. R., Greenspan, P., Galvin, K., Manfredi, M., Claiborne, C., Amidon, B., Bence, N. F. (2018). A small-molecule inhibitor of the ubiquitin activating enzyme for cancer treatment. *Nat Med.* 24(2), 186-193.

Kaganovich, D., Kopito, R., & Frydman, J. (2008). Misfolded proteins partition between two distinct quality control compartments. *Nature*. 454(7208), 1088-1095.

Kim, T. K. & Goldberg, A. L. (2017). The deubiquitinating enzyme USP14 allosterically inhibits multiple proteasomal activities and ubiquitin-independent proteolysis. *J Biol Chem*. 292(23), 9830-9839.

Kim, W., Bennet, E. J., Huttlin, E. L., Guo, A., Li, J., Possemato, A., Sowa, M. E., Rad, R., Rush, J., Comb, M. J., Harper, J. W., & Gygi, S. P. (2011). Systematic and quantitative assessment of the ubiquitin-modified proteome. *Mol Cell,* 44(2), 325-340.

Kisselev, A. F., Callard, A., & Goldberg, A. L. (2006). Importance of the Different Proteolytic Sites of the Proteasome and the Efficacy of Inhibitors Varies with the Protein Substrate. *J Biol Chem*.281(13), 8582-8590.

Lee, B., Lu, Y., Prado, M. A., Shi, Y., Tian, G., Sun, S., Elsasser, S., Gygi, S. P., King, R. W., Finley, D. (2016). USP14 deubiquitinates proteasome-bound substrates that are ubiquitinated at multiple sites. *Nature*. 532(7599), 398-401.

Messick, T. E., & Greenberg, R. A. (2009). The ubiquitin landscape at DNA double-strand breaks. *J. Cell Biol.,* 187(3), 319-326.

Nawrocki, S. T., Carew, J. S., Dunner, K., Boise, L. H., Chiao, P. J., Huang, P., Abbruzzese, J.L., McConkey, D.J. (2005). Bortezomib inhibits PKR-like endoplasmic reticulum (ER) kinase and induces apoptosis via ER stress in human pancreatic cancer cells. *Cancer Res,* 65(24), 11510-11519.

Obeng, E. A., Carlson, L. M., Gutman, D. M., Harrington, W. J., Lee, K. P., & Boise, L. H. (2006). Proteasome inhibitors induce a terminal unfolded protein response in multiple myeloma cells. *Blood*, 107, 4907–4916.

Reyes Turcu F. E., Ventii K. H., & Wilkinson K. D. (2009). Regulation and Cellular Roles of Ubiquitin-specific Deubiquitinating Enzymes. *Annu Rev Biochem,* 78, 363-397.

Ri, M. (2016). Endoplasmic‐reticulum stress pathway‐associated mechanisms of action of proteasome inhibitors in multiple myeloma. *Int J Hematol,* 104, 273-280.

Rogov V., Dotsch, V., Johansen T., and Kirkin V. (2014) Interactions between autophagy receptors and ubiquitin-like proteins form the molecular basis for selective autophagy. *Mol. Cell.* 53, 167-178.

Sanchez-Lanzas, R., and Castano, J. G. (2014). Proteins Directly Interacting with Mammalian 20S Proteasomal Subunits and Ubiquitin-Independent Proteasomal Degradation. *Biomolecules,* 4(4), 1140-11054.

Schulman, B. A. & Harper, J. W. (2009). Ubiquitin-like protein activation by E1 enzymes: the apex for downstream signalling pathways. *Nat Rev Mol Cell Biol,* 10(5), 319-331.

Sha Z., Schnell, H. M., Ruoff, K., Goldberg, A. (2018). Rapid induction of p62 and GABARAPL1 upon proteasome inhibition promotes survival before autophagy activation. J. Cell Biol, 217(3).

Soucy, T. A., Smith, P. G., Milhollen, M. A., Berger, A. J., Gavin, J. M., Adhikari, S., Brownell, J. E., Burke, K. E., Cardin, D. P., Critchley, S., Cullis, C. A., Doucette, A., Garnsey, J. J., Gaulin, J. L., Gershman, R. E., Lublinsky, A. R., McDonald, A., Mizutani, H., Narayanan, U., Olhava, E. J., Peluso, S., Rezaei, M., Sintchak, M.D., Talreja, T., Thomas, M.P., Traore, T., Vyskocil, S., Weatherhead, G.S., Yu, J., Zhang, J., Dick, L. R., Claiborne, C. F., Rolfe, M., Bolen, J. B., & Langston, S. P. (2009). An inhibitor of NEDD8-activating enzyme as a new approach to treat cancer. *Nature*, 458(7239), 732-6.

Swatek, K. & Komander, D. (2016). Ubiquitin modifications. *Cell Research*, 26, 399-422.

VELCADE® (bortezomib) | How VELCADE works. (2016). Retrieved from VELCADE® (bortezomib): http://www.velcade.com/understanding-velcade/about-velcade

Wang, B., Ma, A., Zhang, L., Jin, W. L., Qian, Y., Xu, G., Qiu, B., Yang, Z., Liu, Y., Xia, Q., & Liu, Y. (2015). POH1 deubiquitilates and stabilizes E2F1 to promote tumour formation. *Nat Commun,* 6(8704), 1-15.

What Is Multiple Myeloma? (2018). Retrieved from American Cancer Society: http://www.cancer.org/cancer/multiplemyeloma/detailedguide/multiple-myeloma-what-is-multiple-myeloma